SPIN CONFIGURATIONS OF MAGNETIC IONS ON B-SITES IN NORMAL CUBIC SPINELS

Toshiro Akino

Synopsis

Possible ground-state spin configurations in normal cubic spinels having magnetic ions on B-sites only are studied with the assumption of four superexchange interactions. Spin configurations are constructed using one wavevector or two wavevectors restricted along one of [001], [110], and [111], and their stability is studied with respect to wavevectors in the whole Brillouin zone. It is shown that a helix with a wavevector (0,0,k) is stable in a certain region in the exchange-parameter space. Two helices, with (k,k,0) and (k,k,k), and the Yafet-Kittel type configuration have lower energies than all other constructed configurations in certain regions, but they are not the ground state. A cone-helix along [110] having a conical structure in two sublattices and a coplanar structure in the other two sublattices has the lowest energy in a large region of the parameter space among all the configurations constructed with two wavevectors. Relevant observed spin structures in chromium chalcogenide spinels, MgV_2O_4, $GeCo_2O_4$, and $GeNi_2O_4$, are discussed.

Spin configurations with the wavevector $(2\pi/a,0,\pi/a)$ of the neutron diffraction pattern for $ZnFe_2O_4$ are also constructed with the assumption of five different superexchange interactions, and their stability is studied. It is shown that three types of degenerate antiferromagnetic configurations are the ground spin state on a straight line in the two-dimensional exchange-parameter space at fixed values of the other two parameters. Magnetic dipole-dipole interaction stabilizes four particular noncollinear antiferromagnetic configurations and gives a width to the line of stability. These four configurations give the same neutron diffraction line intensities which are in fairly good agreement with the observed intensities due to König et al..

Acknowlegments

The auther would like to express his sincere gratitude to Professor T. Nagamiya and Professor K. Motizuki for continuous guidance and valuable discussion as well as for improving the manuscript. Without their encouragement this work would not have been completed. He is also indebted to Dr. S. Takeuchi for helpful discussion.

Contents

INTRODUCTION

Normal cubic spinels with nonmagnetic cations on A-sites and magnetic cations on B-sites are of interest in the study of B-B interactions. Early in 1956, Anderson showed that nearest-neighbor interactions alone cannot produce any long-range order on B-sites. Subsequently, Hastings and Corliss observed a complicated neutron diffraction pattern for $ZnFe_2O_4$ at 2.7 K whose main peak corresponded to a wavevector $(2\pi/a,0,\pi/a)$, but the spin structure was not determined due to lack of resolution. Recently König et al. observed well-resolved magnetic peaks up to high diffraction angles for $ZnFe_2O_4$ at 4.2 K, and these peaks again corresponded to $(2\pi/a,0,\pi/a)$. Up to the present time numerious experimental investigations have been done on the spin structures of the spinels having magnetic cations on B-sites only, especially those of chromium chalcogenide spinels, by magnetic measurments and neutron diffraction observations. The compounds $CdCr_2S_4$, $CdCr_2Se_4$, and $HgCr_2Se_4$ have been found to be ferromagnetic. Neutron diffraction studies showed that the compounds $ZnCr_2Se_4$ and $HgCr_2S_4$ have spin arrangements of the (0,0,k) type helix and that the compounds MgV_2O_4, $MgCr_2O_4$, $GeCo_2O_4$, and $GeNi_2O_4$ have complicated antiferromagnetic spin structures. For the (0,0,k) helical ground state in $ZnCr_2Se_4$ Dwight and Menyuk made a theoretical analysis on the basis of nearest-neighbor and five distant-neighbor interactions. They used the method of Lyons and Kaplan to delineate the stability region of the (0,0,k) helical ground state in the exchange-parameter space, using two relations that were determined from experimental data among five exchange ratios.

In the situation mentioned above we study in the present work various theoretically possible ground-state spin configurations at T = 0 in normal cubic spinels having magnetic cations on B-sites only. The contents of this work are divided into two parts:

Part I: [001], [110], and [111] Spin Configurations,

Part II: Theory of Magnetic Structure of Zinc Ferrite.

In Part I we construct spin configurations having one wavevector or two wavevectors restricted along one of [001], [110], and [111], under the assumption of four different superexchange interactions, and we study their stability with respect to all wavevectors in the whole Brillouin zone. The Lyons-Kaplan theory, described concisely by Nagamiya, is used. Relevant observed spin structures are discussed.

In Part II we construct spin configurations with a wavevector $(2\pi/a,0,\pi/a)$ found in the neutron diffraction pattern for $ZnFe_2O_4$, under the assumption of five different superexchange interactions, and we study their stability. We find new degenerate antiferromagnetic configurations. We further study the effect of magnetic dipole-dipole interaction stabilizing particular ones of these antiferromagnetic configurations.

Part I

[001], [110], and [111] Spin Configurations

§1. Introduction

The magnetic properties of the normal cubic spinels having nonmagnetic cations on A-sites and magnetic cations on B-sites, especially chromium chalcogenide spinels, have been investigated by several workers. It was found that $ZnCr_2Se_4$[1),2)] has a spin arrangement of the (0,0,k) helix type, with a turn angle of 42° at 4.2°K, and a positive asymptotic paramagnetic Curie temperature of 115°K. Lotgering accounted for these properties assuming a strong ferromagnetic nearest-neighbor Cr-Se-Cr superexchange interaction, with positive J_0, and relatively weak antiferromagnetic second, third, and fourth neighbor superexchange interactions via anions, with negative J_1, J_2, J_3. Plumier considered only three interactions assuming $J_3 = 0$ and determined the other constants uniquely from experimental results as $J_0 = 24.9°K$, $J_1 = 7.8°K$, and $J_2 = -10.65°K$.

The compounds $CdCr_2S_4$, $CdCr_2Se_4$, $HgCr_2S_4$, and $HgCr_2Se_4$[3),4)] were found to be ferromagnetic, with Curie temperatures of 84.5, 129.5, 36.0, and 106°K, respectively. All these materials except $HgCr_2S_4$ are ferromagnetic at least down to 4.2°K, whereas $HgCr_2S_4$ was observed to be metamagnetic below 25°K. Neutron diffraction experiment by Hastings and Corliss[5)] showed, however, that the spin structure of $HgCr_2S_4$ at low temperatures is a (0,0,k) helix, with a turn angle of 22° at 6.5°K, which decreases with increasing temperature, reaching a value of 10° at 30°K, beyond which it shows little variation up to 60°K, the Néel point observed by this experiment. For the ferromagnetic spinels, Baltzer et al.[4)] made a theoretical analysis under the assumption that antiferromagnetic distant-neighbor interactions occur exclusively via the A-site cations.

A rigorous analysis of the (0,0,k) helical ground state for $ZnCr_2Se_4$ was made by Dwight and Menyuk[6)] on the basis of nearest-neighbor and

five distant-neighbor interactions. They used the method of Lyons and Kaplan[7] to delineate the stability region of the (0,0,k) helical ground state in the exchange-parameter space, using two relations, determined from experimental data, among the five exchange ratios. They pointed out that the model proposed by Baltzer et al. for chalcogenide spinels is not justifiable.

In addition to chromium chalcogenide spinels, neutron diffraction studies have been made for $ZnFe_2O_4$,[8] $GeCo_2O_4$,[9] $GeNi_2O_4$,[10] MgV_2O_4,[11] and $MgCr_2O_4$,[12),13] for which some complicated antiferromagnetic spin configurations have been inferred from the experimental results.

In the situation mentioned above, we study in the present Part I various theoretically possible ground spin configurations at T=0 in the normal cubic spinel having magnetic cations on B-sites only. We restrict ourselves to four superexchange interactions via two anions, with exchange constants J_0, J_1, J_2, and J_3. We neglect the interaction B-anion-A-anion-B, the inclusion of which would require the division of J_2 into J_2' and J_2'', and also neglect interactions via three or more anions. The Lyons-Kaplan theory, described concisely by Nagamiya,[14] is used.

§2. Formulation

We consider a normal cubic spinel whose A-sites are occupied by nonmagnetic ions and B-sites by magnetic ions. We can choose a rhombohedral unit cell which contains four B-site ions,

1. (0,0,0), 2. (0,a/4,a/4), 3. (a/4,a/4,0), 4. (a/4,0,a/4),

described in cubic coordinates, where a is the lattice constant; see Fig.1. Let $S_{n\nu}$ be the classical spin vector of the νth magnetic ion in the nth unit cell and $R_{n\nu}$ its position. The exchange energy can be written as

$$E = -\sum_{m,\mu}\sum_{n,\nu} J(R_{m\mu,n\nu})S_{m\mu}\cdot S_{n\nu} \qquad (R_{m\mu,n\nu} = R_{m\mu} - R_{n\nu}). \tag{2.1}$$

Using the Fourier transforms of $J(R_{m\mu,n\nu})$ and $S_{m\mu}$,

$$C_{\mu\nu}(q) = -\sum_{m} J(R_{m\mu,n\nu})\exp(-iq\cdot R_{m\mu,n\nu}), \tag{2.2}$$

$$\sigma_{q\mu} = (SN)^{-1}\sum_{m} S_{m\mu}\exp(-iq\cdot R_{m\mu}), \tag{2.3}$$

where S is the magnitude of the spin vector on each B-site and N the number of unit cells, Eq.(2.1) becomes

$$E/NS^2 = \sum_{q,\mu,\nu} C_{\mu\nu}(q)\sigma_{q\mu}\cdot\sigma_{-q\nu}. \tag{2.4}$$

We may consider exchange interactions of six kinds, particularly for chalcogenide spinels in which the crystalline binding may involve a large covalency: J_0 between nearest neighbours, J_1 between (0,0,0) and (a/2,-a/4,a/4) (and for equivalent pairs), J_2' between (0,0,0) and (a/2,a/2,0), J_2'' between (0,0,0) and (a/2,-a/2,0), J_3 between (0,0,0) and (3a/4,-a/4,0), and J_4 between (0,0,0) and (a,0,0); see Fig.1. If we write

$$J_2' = J_2(1 - \gamma) \quad \text{and} \quad J_2'' = J_2(1 + \gamma), \tag{2.5}$$

then γ is a quantity that represents the degree of covalency of the A-site cations. However, for most part of the present Part I we put $\gamma = 0$ and $J_4 = 0$. These quantities, γ and J_4, will appear only in our qualitative discussion. Different notation for the interaction constants due to various investigators is listed in Table 1. We also write $\xi = J_0/J_2$, $\eta = J_1/J_2$, $\zeta = J_3/J_2$, and measure q in units of 4/a.

The diagonal elements of the matrix $[C_{\mu\nu}(q_x,q_y,q_z)]$ can be written as

$$C_{11}(q_x,q_y,q_z) = C_{22}(q_x,q_y,q_z) = C_{33}(q_x,q_y,q_z) = C_{44}(q_x,q_y,q_z)$$
$$= -2J_2\{\cos2(q_x + q_y) + \cos2(q_y + q_z) + \cos2(q_z + q_x) + \cos2(q_x - q_y)$$
$$+ \cos2(q_y - q_z) + \cos2(q_z - q_x)\}, \qquad (2.6)$$

and the off-diagonal elements are as follows:

$$C_{12}(q_x,q_y,q_z) = -2J_2[\xi\cos(q_y + q_z) + \eta\{\cos(2q_x + q_y - q_z)$$
$$+ \cos(2q_x - q_y + q_z)\} + \zeta\{\cos(3q_y - q_z) + \cos(q_y - 3q_z)\}], \qquad (2.7a)$$

$$C_{13}(q_x,q_y,q_z) = C_{12}(q_z,q_y,q_x), \qquad (2.7b)$$

$$C_{14}(q_x,q_y,q_z) = C_{12}(q_y,q_x,q_z), \qquad (2.7c)$$

$$C_{23}(q_x,q_y,q_z) = C_{12}(q_y,q_x,-q_z), \qquad (2.7d)$$

$$C_{24}(q_x,q_y,q_z) = C_{12}(q_z,-q_y,q_x), \qquad (2.7e)$$

$$C_{34}(q_x,q_y,q_z) = C_{12}(q_x,q_y,-q_z). \qquad (2.7f)$$

The matrix is symmetric:

$$C_{\mu\nu}(q_x,q_y,q_z) = C_{\nu\mu}(q_x,q_y,q_z) \qquad (2.8)$$

Our mathematical problem is to look for the lowest minimum of the exchange energy given by Eq.(2.4) subject to the condition

$$S_{n\nu}^2 = S^2 \qquad \text{for all n and } \nu.$$

This condition can be written as

$$\sum_q \sigma_{q\nu}\sigma_{-q\nu} = 1 \qquad (\nu = 1,2,3,4), \tag{2.9a}$$

$$\sum_q \sigma_{q\nu}\sigma_{q'-q\nu} = 0 \qquad \text{for all } q' \neq 0. \tag{2.9b}$$

In the following we sketch the method described in Ref.14, since it forms the basis of the present study. We introduce arbitrary parpmeters β_ν and consider in place of (2.9a) the following condition:

$$\sum_\nu \sum_q \beta_\nu^{-2}\sigma_{q\nu}\sigma_{-q\nu} = \sum_\nu \beta_\nu^{-2}. \tag{2.10}$$

Introducing the Lagrange multiplier λ, we minimize the exchange energy (2.4) subject to the condition (2.10). Then we have the eigenvalue equation:

$$\sum_\mu C_{\mu\nu}(q)\,\sigma_{q\mu} = \lambda\beta_\nu^{-2}\sigma_{q\nu} \qquad (\nu = 1,2,3,4) \tag{2.11}$$

from which we obtain eigenvalues and eigenvectors for given q and β_ν. If we take a spin configuration represented by a pair of inequivalent wavevectors q and -q and take account of the condition (2.9b), then we have

$$\sigma_{q\nu} = \frac{1}{2}(\hat{i} - i\hat{j})u_{q\nu}, \tag{2.12}$$

where $\hat{i}$ and $\hat{j}$ are orthogonal unit vectors which are independent of ν.*) From (2.9a) it follows that

$$|u_{q\nu}| = 1. \tag{2.13}$$

---

*) When q and -q are equivalent to each other, $\sigma_{q\nu}$ takes the form $\sigma_{q\nu} = u_{q\nu}\hat{i}$ with $|u_{q\nu}| = 1$.

The ratio of $u_{q\nu}$ is determined from the same equations as (2.11), i.e., from

$$\sum_{\mu} C_{\mu\nu}(q)u_{q\mu} = (\lambda \beta_{\nu}^{-2})u_{q\nu} \qquad (\nu = 1,2,3,4). \tag{2.14}$$

The parameters β_{ν} are so chosen that the condition (2.13) is satisfied for all ν. The lowest eigenvalue is denoted by $\lambda_0(Q)$, q being written as Q. It then follows that the corresponding spin configuration gives the absolute minimum of the exchange energy. It was proved[15] that, if the eigenvalue of a coplanar configuration is not the lowest of all eigenvalues including those for $q \neq Q$ (but with fixed β_{ν}), this configuration is locally unstable and cannot be the ground spin state. Eq.(2.4) can be written as

$$E/NS^2 = \lambda_0(Q)\sum_{\nu} \beta_{\nu}^{-2}. \tag{2.15}$$

When we fail to find a solution with $\pm$ Q only, we may take another wavevector Q' besides Q. If Q is a general wavevector, Q' must be one of 0, K/2, and K/4 in order that the condition (2.9b) be satisfied, where K is a reciprocal vector. Besides Eq.(2.12), we have

$$\sigma_{Q'\nu} = u_{Q'\nu}\hat{k} \qquad \text{if } Q' = 0 \text{ or } K/2, \tag{2.16}$$

where $u_{Q'\nu}$ is determined from Eq.(2.14) with Q' in place of Q and $\hat{k}$ is the unit vector perpendicular to both $\hat{i}$ and $\hat{j}$. Furthermore the condition (2.9a) can be written as

$$|u_{Q\nu}|^2 + |u_{Q'\nu}|^2 = 1. \tag{2.17}$$

The parameters β_{ν} are so chosen that the eigenvalues for the two wavevectors are the same and the lowest, and that the condition (2.17) is satisfied for all ν.

§3. (0,0,k) Spin Configurations

We consider first spin configurations having only one wavevector $q = (0,0,k)$, measuring k in units of $4/a$ as before. The matrix $[C_{\mu\nu}(k)]$, where we abbreviate $C_{\mu\nu}(0,0,k)$ as $C_{\mu\nu}(k)$, has the symmetry $C_{12}(k) = C_{14}(k) = C_{23}(k) = C_{34}(k)$ and $C_{13}(k) = C_{24}(k)$. In this case we can choose $\beta_1 = \beta_2 = \beta_3 = \beta_4 = 1$. Under a unitary transformation

$$X_1 = (u_1 + u_2 + u_3 + u_4)/2, \quad X_2 = (u_1 + u_2 - u_3 - u_4)/2,$$
$$X_3 = (u_1 - u_2 + u_3 - u_4)/2, \quad X_4 = (u_1 - u_2 - u_3 + u_4)/2, \tag{3.1}$$

the eigenvalue equation (2.14) can be put into diagonal form.

For X_1 we obtain

$$\lambda_1^{[001]}(k) = C_{11}(k) + C_{13}(k) + 2C_{12}(k), \quad u_1=u_2=u_3=u_4, \tag{3.2}$$

for X_2 and X_4 we have

$$\lambda_2^{[001]}(k) = \lambda_4^{[001]}(k) = C_{11}(k) - C_{13}(k), \quad u_1=-u_3, \; u_2=-u_4, \tag{3.3}$$

and for X_3 we have

$$\lambda_3^{[001]}(k) = C_{11}(k) + C_{13}(k) - 2C_{12}(k), \quad u_1=-u_2=u_3=-u_4. \tag{3.4}$$

However, the configuration for λ_3 is equivalent to that for λ_1 as k may be replaced by $\pi - k$. Looking for the minimal eigenvalues of the above λ's, we obtain following six possible configurations:

(a) Ferromagnetic configuration ($k = 0$, $u_1 = u_2 = u_3 = u_4$)

$$\lambda_1^{[001]}(0) = -6J_2(\xi + 2\eta + 2\zeta + 2). \tag{3.5}$$

(b) [001] helical configuration-1 ($0 < k < \pi/2$, $u_1 = u_2 = u_3 = u_4$)

$$\lambda_1^{[001]}(k) = -2J_2[\xi - 2\eta + 2\zeta - 2 + 2(\xi + 2\eta - 2\zeta)\cos k + 4(\eta + 2)\cos^2 k + 8\zeta\cos^3 k], \tag{3.6}$$

where the turn angle k is determined from $d\lambda_1^{[001]}(k)/dk = 0$, i.e., from

$$\cos k = [-(\eta + 2) \mp \sqrt{\{(\eta + 2)^2 - 3\zeta(\xi + 2\eta - 2\zeta)\}}]/6\zeta \quad \text{for } \zeta \neq 0. \tag{3.7}$$

Here the minus sign corresponds to $J_2 > 0$ and the plus sign to $J_2 < 0$. For $\zeta = 0$ we have

$$\cos k = -(\xi + 2\eta)/[4(\eta + 2)]. \tag{3.8}$$

(c) [001] helical configuration-2 ($\pi/2 < k \leq \pi$, $u_1 = u_2 = u_3 = u_4$)

Formulas are the same as those in (b).

(d) Degenerate antiferromagnetic configuration

(d-1) Verwey order type ($k = \pi$, $u_1 = u_2 = u_3 = u_4$)

$$\lambda_1^{[001]}(\pi) = -2J_2(-\xi - 2\eta - 2\zeta + 6). \tag{3.9}$$

The spins on each (001) plane are ordered ferromagnetically, but spins on adjacent planes are antiparallel.

(d-2) Uncorrelated antiferromagnetic structure ($k = 0$, $u_1 = -u_3$, $u_2 = -u_4$)

$$\lambda_2^{[001]}(0) = \lambda_4^{[001]}(0) = -2J_2(-\xi - 2\eta - 2\zeta + 6). \tag{3.10}$$

The spins on sublattice 1 and those on sublattice 3 are antiparallel and the spins on 2 and those on 4 are also antiparallel; in each sublattice the spins are parallel. The spin axis of (1, 3) and that of (2, 4) are, however, uncorrelated.

The ground spin state (d) is indeterminate in cubic spinels, but as was pointed out by Aiyama,[16] the two accidentally degenerate eigenvalues

of (d-1) and (d-2) split if there is a tetragonal distortion. He also pointed out that the ground state of $ZnMn_2O_4$ (c/a = 1.14) is the uncorrelated antiferromagnetic structure.

(e) Uncorrelated antiferromagnetic [001] configuration-1

$$(k = \pi/2,\ u_1 = u_3,\ u_2 = u_4)$$

$$\lambda_1^{[001]}(\pi/2) = \lambda_3^{[001]}(\pi/2) = -2J_2(\xi - 2\eta + 2\zeta - 2). \tag{3.11}$$

The spins on each (001) plane are parallel, but in the pair of sublattices (1, 3), as well as in the pair of sublattices (2, 4), the spin direction alternates by an angle π in going along the [001] axis. The spin axis in (1, 3) and that in (2, 4) are uncorrelated. We shall call this configuration UA1.

(f) Uncorrelated antiferromagnetic [001] configuration-2

$$(k = \pi/2,\ u_1 = -u_3,\ u_2 = -u_4)$$

$$\lambda_2^{[001]}(\pi/2) = \lambda_4^{[001]}(\pi/2) = -2J_2(-\xi + 2\eta - 2\zeta - 2). \tag{3.12}$$

The spins 1 and 3 on each (001) plane are ordered antiparallel and these spins alternate with a turn angle π along the [001] axis. The same is true for the spins 2 and 4, but the spin axis in (1, 3) and that in (2, 4) are uncorrelated (see Fig.2). We call this configuration UA2.

We show in Figs.3, 4, 5 for $\zeta = J_3/J_2 = 1/2,\ 0,\ -1/2$ the regions in the $\xi\eta$ plane ($\xi = J_0/J_2, \eta = J_1/J_2$) in which the above six configurations take their respective lowest eigenvalues. Bold lines represent the boundaries of the configurations (a), (b), (c), (d), and (f), excepting (e). The UA1 configuration is represented by a straight line (e). Dashed lines in the helical regions (b) and (c) represent loci of $k = \pi/3$ and $k = 2\pi/3$. Dwight and Menyuk[6] studied mainly the stability of the helix (b) in $ZnCr_2Se_4$, so that they assumed J_0 to be positive and the largest of all J's. We do

not confine ourselves to such a case and find the possibility of a new spin state UA2.

Next we study the stability of all these configurations, comparing their eigenvalues with eigenvalues for all the wavevectors in the Brillouin zone. Because of the symmetry of $[C_{\mu\nu}(q_x,q_y,q_z)]$, only 1/48 of the first Brillouin zone may be considered. We have investigated the stability with respect to eigenvalues for wavevectors along [110], [111], and [210], and special wavevectors at 22 points shown in Fig.6. We carried out numerical calculations by using a NEAC 2200 computer, and we find the shaded regions in Figs. 3, 4, 5 for the instability of the present [001] configurations. The main features of the stability and instability are as follows.

1) The stability of the ferromagnetic configuration.

In the region where all superexchange constants are positive the ferromagnetic configuration, (a), is stable. When there are negative superexchange constants, this configuration is unstable in a certain small region. For example, in the case of $\zeta = 0$ and $J_2 > 0$ in Fig.4, this configuration is unstable in a small belt-like region (a part of the shaded region above the line $k = 0$ in the quadrant $\xi > 0$, $\eta < 0$) with respect to $q = (\pi/4,\pi/4,\pi/4)$. We may therefore anticipate there a new spin configuration having two wavevectors, $q = 0$ and $q' = (\pi/4,\pi/4,\pi/4)$. This problem will be treated in §5.

2) The stability of the helix [001]-1.

In the case of $\zeta = 1/2$ shown in Fig.3, this configuration is unstable everywhere. In the case of $\zeta = 0$ and $J_2 < 0$, however, a small region in $\xi < 0$, $\eta < 0$ remains the stability region as can be seen in Fig.4 (the white region for (b)). A larger stability region is obtained in the case of $\zeta = -1/2$ and $J_2 < 0$, as shown in Fig.5. It can be concluded that J_2 must be negative in order that the helix [001]-1 is the ground spin configuration,

and also that positive values of J_3 tend to stabilize it ($\zeta = J_3/J_2$).

Plumier[2] found by neutron diffraction that $ZnCr_2Se_4$ has a spin arrangement of the helix [001]-1 type, with a turn angle k=42°. Point P in the stability region in Fig.4 corresponds to exchange constants determined from experimental data by Plumier for $ZnCr_2Se_4$. Dwight and Menyuk[6] concluded, from the Goodenough-Kanamori rules of superexchange that $J_2 < 0$ and $J_3 > 0$ for Cr^{3+} in B-sites. Hence the helix [001]-1 can be expected for chromium spinels, and in fact it was observed in $ZnCr_2Se_4$ and $HgCr_2S_4$.

Furthermore, there is an evidence that the ground spin state of $CdCr_2S_4$ is ferromagnetic[3),4)]. In $CdCr_2S_4$ and $HgCr_2S_4$ the lattice parameter a and the asymptotic paramagnetic Curie temperature Θ are a = 10.244 Å, Θ= 152°K and a = 10.237 Å, Θ = 142°K, respectively, and the u parameter is the same. To explain the difference of the spin structures of $CdCr_2S_4$ and $HgCr_2S_4$, we expect the following inequalities to hold:

$$\xi_{Cd} < \xi_{Hg}, \text{ i.e. } (J_0/|J_2|)_{Cd} > (J_0/|J_2|)_{Hg}, \tag{3.13}$$

$$\eta_{Cd} \lesssim \eta_{Hg}, \text{ i.e. } (J_1/|J_2|)_{Cd} \gtrsim (J_1/|J_2|)_{Hg}, \tag{3.14}$$

$$\zeta_{Cd} \lesssim \zeta_{Hg}, \text{ i.e. } (J_3/|J_2|)_{Cd} \gtrsim (J_3/|J_2|)_{Hg}. \tag{3.15}$$

Here the negative slope of the boundary between (a) and (b) in the case of $J_2 < 0$, $\xi < 0$ and a shift of the boundary in going from $\zeta = 0$ to $\zeta = -1/2$ have been considered. The inequality (3.13) is qualitatively understood from the fact that a chromium chalcogenide spinel having a larger lattice parameter has a larger positive value Θ which is determined mainly by J_0[4)]. It might also be that $|J_2|$ takes a larger value in Hg-compound. The inequality (3.14) is understood from another point of view that, in the case of $\zeta = -1/2$ and $J_2 < 0$ (Fig.5), a change in η ($=J_1/J_2$) near $\eta = 0$ at a fixed negative value of ξ gives rise to the transition

from the ferromagnetic configuration, (a), to the helix [001]-1 configuration, (b). A small difference in η for $CdCr_2S_4$ and $HgCr_2S_4$ can be expected by taking into account their different degrees of A-site covalency. The covalency effect for J_3 might also account for the inequality (3.15). Dwight and Menyuk[6] pointed out that negative values of γ tend to stabilize the helix [001]-1.

3) The stability of the UA2 configuration.

This configuration is unstable for $J_2 > 0$ in the three cases of $\zeta = 1/2$, 0, -1/2. For $\zeta = 1/2$, $J_2 < 0$ and for $\zeta = 0$, $J_2 < 0$, this configuration is stable in the unshaded part of the region marked (f). Hence for the stabilization of the UA2 configuration J_2 must be negative, and J_0 ($= \xi J_2$) and J_3 ($= \zeta J_2$) prefer negative values. Plumier and Tardieu[11] found by neutron diffraction that MgV_2O_4 at 4.2°K has a correlated antiferromagnetic spin arrangement of a wavevector $q = (0,0,\pi/2)$ shown in Fig.7. This compound is tetragonally distorted at low temperatures according to X-ray diffraction[17]. Within our assumption of cubic crystal and four isotropic exchange interactions the ground spin state of MgV_2O_4 must be UA2. Even by taking γ and J_4 into account, we still obtain UA2 (Appendix C). Hence, the observed correlated configuration should be due to an anisotropy energy and the tetragonality.

§ 4. (k,k,0) Spin Configurations

Next we take a wavevector along [110], and we write q = (k,k,0). The off-diagonal elements of the matrix $[C_{\mu\nu}(k)]$, $C_{\mu\nu}(k,k,0)$ being abbreviated as $C_{\mu\nu}(k)$, have the symmetry $C_{12}(k) = C_{14}(k) = C_{23}(k) = C_{34}(k)$. We choose β_ν in such a way that the matrix $[\beta_\mu\beta_\nu C_{\mu\nu}(k)]$ retains the symmetry of $[C_{\mu\nu}(k)]$, i.e., $\beta_1 = \beta_3 = \beta$ and $\beta_2 = \beta_4 = 1$. Under a unitary transformation

$$\begin{aligned} X &= (u_1 + u_3)/\sqrt{2}, \qquad X' = (u_1 - u_3)/\sqrt{2}, \\ Y &= (u_2 + u_4)/\sqrt{2}, \qquad Y' = (u_2 - u_4)/\sqrt{2}, \end{aligned} \tag{4.1}$$

The matrix $[\beta_\mu\beta_\nu C_{\mu\nu}(k)]$ is partially diagonalized into a two-dimensional matrix and two one-dimensional ones. For the former we have the following eigenvalue equation for X and Y:

$$\begin{vmatrix} C_{11}(k) + C_{13}(k) - \lambda/\beta^2 & 2C_{12}(k) \\ 2C_{12}(k) & C_{11}(k) + C_{24}(k) - \lambda \end{vmatrix} = 0. \tag{4.2}$$

Solving Eq.(4.2), we obtain two eigenvalues, of which the lower one is

$$\begin{aligned} \lambda_1^{[110]}(k) = \tfrac{1}{2}[\beta^2(C_{11}(k) + C_{13}(k)) + C_{11}(k) + C_{24}(k) \\ - \sqrt{[\{\beta^2(C_{11}(k) + C_{13}(k)) - C_{11}(k) - C_{24}(k)\}^2 + 16\beta^2 C_{12}(k)^2]}]. \end{aligned} \tag{4.3}$$

For this we have $u_1 = u_3$ and $u_2 = u_4$. From a one-dimensional matrix for X' we have

$$\lambda_2^{[110]}(k) = \beta^2(C_{11}(k) - C_{13}(k)), \qquad u_1 = -u_3, \quad u_2 = u_4 = 0. \tag{4.4}$$

From the other one-dimensional matrix for Y' we have

$$\lambda_3^{[110]}(k) = C_{11}(k) - C_{24}(k), \qquad u_1 = u_3 = 0, \quad u_2 = -u_4. \tag{4.5}$$

We construct the (k,k,0) configurations in the shaded regions of Figs. 3, 4, 5. The details of these configurations are shown in Appendix A. First we consider the following case (g).

(g) Helix [110]

Here the spins on each (110) plane are parallel and the helix propagates in the [110] direction with a turn angle k. We determine k from $d\lambda_1^{[110]}(k)/dk = 0$, using Eq. (4.3). We can choose β so as

$$X/Y = u_1/u_2 = 1, \quad \text{i.e., } u_1 = u_2 = u_3 = u_4$$

is satisfied.

At first we compare the exchange energy of the helix [110] with those of the unstable [001] configurations in the shaded regions of Figs. 3, 4, 5. The result turns out to be that the helix [110] has a lower energy in a region of mostly $\xi < 0$ shown in Fig.8 in the case of $\zeta = 1/2$ and $J_2 < 0$. Next we study its stability. When we calculate eigenvalues for q = (k,k,k) from Eq. (2.14) using the present values of β's, we find that some of them are lower in the whole (g) region. Hence, unfortunately, the coplanar helix [110] cannot be the ground spin state.

In order to fill the shaded regions of Figs. 3, 4, 5, we try to find other solutions. When k is equal to $\pi/2$, we have $C_{12}(\pi/2) = 0$, and hence from Eq. (4.2) we obtain two eigenvalues

$$\lambda_X^{[110]}(\pi/2) = -2J_2\beta^2(-\xi + 2\eta - 2\zeta - 2), \quad u_1 = u_3, \quad u_2 = u_4 = 0, \tag{4.6}$$

$$\lambda_Y^{[110]}(\pi/2) = -2J_2(\xi - 2\eta + 2\zeta - 2), \quad u_1 = u_3 = 0, \quad u_2 = u_4. \tag{4.7}$$

Furthermore, we have from Eq. (4.4)

$$\lambda_2^{[110]}(\pi/2) = -2J_2\beta^2(\xi - 2\eta + 2\zeta - 2), \quad u_1 = -u_3, \quad u_2 = u_4 = 0, \tag{4.8}$$

and from Eq. (4.5)

$$\lambda_3^{[110]}(\pi/2) = -2J_2(-\xi + 2\eta - 2\zeta - 2), \quad u_1 = u_3 = 0, \quad u_2 = -u_4. \tag{4.9}$$

It is impossible to construct in each case a real configuration with a single wavevector q = $(\pi/2,\pi/2,0)$, because the condition (2.13) cannot be satisfied. However, we can construct spin configurations with two wavevectors, Q = (k,k,0) for $\lambda_1^{[110]}(k)$ of Eq. (4.3), with $d\lambda_1^{[110]}(k)/dk = 0$, and Q' = $(\pi/2,\pi/2,0)$ for one of $\lambda_j^{[110]}(\pi/2)$ (j= x, y, 2, and 3).*) Q' is equivalent to $(0,0,\pi/2)$ and it is one of K/2's. Among four possible configurations, two for j = 2 and 3 have lower energies than the unstable [001] configurations in most part of the shaded regions as described below.

(h) Cone-helix [110]-A

We force degeneracy of two eigenvalues $\lambda_1^{[110]}(k)$, with $u_1(k) = u_3(k)$ and $u_2(k) = u_4(k)$, and $\lambda_2^{[110]}(\pi/2)$, with $u_1(\pi/2) = -u_3(\pi/2)$ and $u_2(\pi/2) = u_4(\pi/2) = 0$. In order to satisfy the condition (2.17), we require

$$|u_2(k)| = 1, \qquad |u_1(k)|^2 + |u_1(\pi/2)|^2 = 1. \tag{4.10}$$

The superposition of the eigenvector $\{\sigma_\nu(k)\}$ based on $(\hat{i}, \hat{j})$ as in Eq. (2.12) and the eigenvector $\{\sigma_\nu(\pi/2)\}$ based on $\hat{k}$ as in Eq. (2.16) yields a cone-helix [110]-A shown in Fig. 9, in which spins on sublattices 1 and 3 have a conical structure and spins on 2 and 4 form a planar helix.

(i) Cone-helix [110]-B

We force degeneracy of two eigenvalues $\lambda_1^{[110]}(k)$ and $\lambda_3^{[110]}(\pi/2)$. From the condition (2.17), we require

$$|u_1(k)| = 1, \qquad |u_2(k)|^2 + |u_2(\pi/2)|^2 = 1. \tag{4.11}$$

We show this cone-helix [110]-B in Fig. 10, in which spins on sublattices 1 and 3 have a planar helical structure and spins on 2 and 4 form a cone.

---

*) It is also possible to construct a spin configuration represented by two wavevectors Q = (k,k,0) and Q' = 0, but this configuration has a high energy.

By computer calculations the energies of the cone-helices [110]-A and B were compared to those of the unstable [001] configurations in the shaded regions of Figs. 3, 4, 5. It was found that the cone-helix [110]-A has a lower energy in most part of the unstable regions for the helix [001] (b) and (c). The cone-helix [110]-B has a lower energy in most part of the unstable regions for UA2, that is (f). The boundaries of the regions of lower energy are shown by chain lines in Figs. 8, 11, 12.

Next we study the stability of these configurations. Since eigenvalues of the matrix $[\beta_\mu \beta_\nu C_{\mu\nu}(q_x,q_y,q_z)]$, with $\beta_1 = \beta_3 = \beta$, $\beta_2 = \beta_4 = 1$, are not affected by reversing the sign of any of q_x, q_y, q_z and by exchanging q_x with q_y, it is sufficient to consider only 1/16 of the first Brillouin zone as shown in Fig. 6.

The results are as follows:

(1) The eigenvalue of the cone-helix [110]-A is higher than the eigenvalue for $q=(\pi/2,\pi/4,0)$, which is one of K/4, in the (h) region of Fig.8 for $\zeta=1/2$, $J_2<0$ and in the corresponding region for $\zeta=-1/2$, $J_2>0$, not shown in figures. We have the same situation for the cone-helix [110]-B in the cases of $\zeta=1/2$, $J_2>0$ and $\zeta=-1/2$, $J_2<0$. The instability against $(\pi/2,\pi/4,0)$ suggests the construction of a configuration having a single wavevector $(\pi/2,\pi/4,0)$ or two wavevectors of which one is this. Hastings and Corliss[8] observed a complicated neutron diffraction pattern for $ZnFe_2O_4$ at 2.7°K whose main peak corresponds to $(\pi/2,\pi/4,0)$.*) In $MgCr_2O_4$ the observed low-temperature reflections correspond to $(\pi/2,\pi/4,0)$ and $(\pi/4,\pi/4,0)$.[13]

---

*) In a recent experiment, well resolved magnetic peaks were observed for $ZnFe_2O_4$ at 4.2K (U. König et al.: Solid State Communications 8 759 (1970)). We discuss the corresponding structure in Part II.

(2) The eigenvalues of the cone-helices [110]-A and B having (k,k,0) for the helical part are higher than those for wavevectors q in the vicinity of (k,0,k) and in the vicinity of (π/2,k,k) in the remaining regions of their lower energies, i.e., the (h) region for ζ=1/2, J_2>0 and for ζ=-1/2, J_2<0, the (i) region for ζ=1/2, J_2<0 and for ζ=-1/2, J_2>0 (see Fig. 11), and both the (h) and (i) regions for ζ=0, J_2>0 and ζ=0, J_2<0 (see Fig. 12). "Bad" wavevectors that upset the stability of the cone-helix [110]-B, for example at points (-6.0, 2.0) and (-6.0,3.5) in the $\xi\eta$ plane in the case of ζ=0 and J_2>0, are shown in Fig. 13. However, "good wavevectors", including zero wavevector, all of K/2, and all of K/4, that stabilize the cone-helix [110]-A or B fill most part of the Brillouin zone.

In the case of non-coplanar cone-helices [110]-A and B, the existence of lower eigenvalues does not necessarily exclude the possibility of their being the ground state, although their stability is not ensured. Kaplan's ferrimagnetic cone structure for the normal cubic spinels having magnetic cations on both A and B sites is in a similar situation, in that "bad wavevectors" exist in the vicinity of <110>.[15)]

§5. Construction of (k,k,k) Spin Configurations

In this section, we restict the wavevector to q=(k,k,k). The matrix $[C_{\mu\nu}(k,k,k)]$, abbreviated as $[C_{\mu\nu}(k)]$, has the symmetry $C_{12}(k) = C_{13}(k) = C_{14}(k)$, $C_{23}(k) = C_{24}(k) = C_{34}(k)$, so that we can choose $\beta_1 = \beta$ and $\beta_2 = \beta_3 = \beta_4 = 1$. Under a unitary transformation

$$\begin{aligned} x &= (u_1 + u_3 + u_4)/\sqrt{3}, \\ y &= (u_2 + u_3 + \omega^2 u_4)/\sqrt{3}, \qquad \omega = \exp(i2\pi/3) \\ z &= (u_2 + \omega^2 u_3 + u_4)/\sqrt{3}, \end{aligned} \tag{5.1}$$

the matrix $[\beta_\mu \beta_\nu C_{\mu\nu}(k)]$ is partially diagonalized into a two-dimensional matrix and two one-dimensional matrices. We have the eigenvalue equation for u_1 and x:

$$\begin{vmatrix} C_{11}(k) - \lambda/\beta^2 & \sqrt{3}C_{12}(k) \\ \sqrt{3}C_{12}(k) & C_{11}(k) + 2C_{23}(k) - \lambda \end{vmatrix} = 0. \tag{5.2}$$

The lower one of the two eigenvalues from Eq. (5.2) is

$$\begin{aligned} \lambda_1^{[111]}(k) = \tfrac{1}{2}[&C_{11}(k) + 2C_{23}(k) + \beta^2 C_{11}(k) \\ &- \sqrt{\{C_{11}(k) + 2C_{23}(k) - \beta^2 C_{11}(k))^2 + 12\beta^2 C_{12}(k)^2\}}], \end{aligned} \tag{5.3}$$

for which $u_2 = u_3 = u_4$. For either y or z we have

$$\lambda_2^{[111]}(k) = C_{11}(k) - C_{23}(k), \tag{5.4}$$

with $u_1 = 0$ and $u_2 + u_3 + u_4 = 0$. We consider (k,k,k) configurations in the shaded regions of Figs. 3, 4, 5 (for details, see Appendix B). First we consider the following case (j).

(j) Helix [111]

Here spins on each (111) plane are parallel and the helix propagates along the [111] axis with a turn angle 2k. We determine k from $d\lambda_1^{[111]}(k)/dk = 0$, using Eq. (5.3). We can choose β so that

$$u_1/x = u_1/\sqrt{3}u_2 = 1/\sqrt{3}, \text{ i.e., } u_1 = u_2 = u_3 = u_4$$

is satisfied.

Comparing the energy of the helix [111] with the energies of the cone-helix [110] A and B and those of the unstable [001] configurations, we find that the helix [111] has a lower energy in the case of $\zeta = 1/2$ and $J_2 < 0$ in a region shown in Fig. 8. With regard to its stability, we calculated eigenvalues for $q = (0,0,k)$ varying k and found some bad wavevectors in the whole (j) region in Fig. 8. Therefore the coplanar helix [111] cannot be the ground state.

For $k = \pi/4$ we have $C_{12}(\pi/4) = 0$ in Eq. (5.2) and hence we have

$$\lambda^{[111]}(\pi/4) = \beta^2 C_{11}(\pi/4) = 0 \tag{5.5}$$

for $u_1 \neq 0$, $u_2 = u_3 = u_4 = 0$. Also, we have

$$\lambda_x^{[111]}(\pi/4) = -4J_2(\xi - 2\zeta) \tag{5.6}$$

for $u_1 = 0$, $u_2 = u_3 = u_4 \neq 0$. Evidently it is impossible to construct a real configuration for each of these eigenvalues.

In order to fill the regions in which the [001] configurations are unstable with respect to $q = (\pi/4,\pi/4,\pi/4)$ (for example, the shaded parts of (a), (b), and (d) ($\xi > 0$, $\eta < 0$) in Fig. 4 for $\zeta = 0$ $J_2 > 0$), we construct a configuration having two wavevectors $Q = 0$ and $Q' = (\pi/4,\pi/4,\pi/4)$ as follows.*)

---

*) Q' is one of K/2. The configuration having $Q = (k,k,k) = 0$ and $Q' = (\pi/4, \pi/4, \pi/4)$ has a higher energy than the unstable [001] configurations in Figs. 3, 4, 5.

(k) Yafet-Kittel-like [111] configuration

We force degeneracy of $\lambda_1^{[111]}(0)$ from Eq. (5.3) and $\lambda_x^{[111]}(\pi/4)$ from Eq. (5.6). From the condition (2.17), we require

$$|u_1(0)| = 1, \qquad |u_2(0)|^2 + |u_2(\pi/4)|^2 = 1. \tag{5.7}$$

Then we have the Yafet-Kittel-like [111] configuration in four (111) layers as shown in Fig. 14.

The region of lower energy of this configuration is shown in Figs. 11 and 12. In the study of the stability of this configuration we note that the axis [111] is not equivalent to the axes $[\bar{1}11]$, $[1\bar{1}1]$, and $[11\bar{1}]$ because of the symmetry of $[\beta_\mu \beta_\nu C_{\mu\nu}(q)]$ for $\beta_1 = \beta$ and $\beta_2 = \beta_3 = \beta_4 = 1$. By computer calculation it was found that this configuration is unstable with respect to wavevectors around $q = (k, -k, k)$ and in particular to $q = (\pi/4, -\pi/4, \pi/4)$. Hence, this coplanar configuration is not the ground state.

Bertaut and his co-workers found for $GeCo_2O_4$ [9] and $GeNi_2O_4$ [10] by neutron diffraction at 4.2°K that in the structure of alternating (111) planes, consisting of (1) and (2, 3, 4), the spins on each (111) plane are parallel but they turn by π in going to every other (111) plane, and the spin axis of (1) and that of (2, 3, 4) are not correlated. This configuration may be called the uncorrelated antiferromagnetic [111] configuration. In order to obtain this configuration, we take a wavevector $q = (\pi/4, \pi/4, \pi/4)$ and force degeneracy of two eigenvalues $\lambda^{[111]}(\pi/4)$ for $u_1 \neq 0$ and $\lambda_x^{[111]}(\pi)$. However, since $C_{11}(\pi/4) = 0$ by Eq. (5.5), the exchange energy is zero and hence is high. Thus, in our approximation of $\gamma = J_4 = 0$ the uncorrelated antiferromagnetic [111] configuration cannot be the ground state. If, however, the Ge^{2+} ions on A-sites have a large covalency and we may take nonzero γ and J_4. Then we obtain following equations (see Appendix C):

$$\lambda^{[111]}(\pi/4) = -6\beta^2(2J_2\gamma - J_4) \qquad (u_1 \neq 0), \tag{5.5'}$$

$$\lambda_x^{[111]}(\pi/4) = -4J_2(\xi - 2\zeta - \gamma) + 6J_4, \tag{5.6'}$$

$$\beta^2 = \frac{2J_2(\xi - 2\zeta - \gamma) + 3J_4}{3(2J_2\gamma - J_4)}. \tag{5.8}$$

The corresponding uncorrelated antiferromagnetic [111] configuration could possibly be the ground state.

§6. Summary

We have assumed the Heisenberg model with four different superexchange constants for normal cubic spinels having nonmagnetic ions on A-sites and magnetic ions on B-sites. We first constructed [001] spin configurations having only one wavevector q = (0,0,k) and studied their stability with respect to wavevectors in the whole Brillouin zone. It was shown that for the stability of a helix with $0 \leq k < \pi/2$, which has been observed in some chromium chalcogenide spinels, J_2 must take negative values and for J_3 positive values are preferred. For uncorrelated antiferromagnetic configuration UA2, described in (f) of Sec.3, J_2 must be negative, and for J_0 and J_3 positive values are preferred. It was shown that within our treatment the ground spin state of MgV_2O_4 cannot be but the UA2 configuration, although actually the spins are correlated (Fig.7), possibly due to a tetragonal distortion. Next we constructed, in the regions of the instability of the [001] configurations in the exchange-parameter space, other configurations which have one wavevector or two wavevectors restricted along [001], [110], and [111] and whose energies are lower than those of the [001] configurations. It was shown that three coplanar configurations, helix [110], helix [111], and a Yafet-Kittel-like [111] configuration, have lower energies than those of all other constructed configurations in certain limited regions. But it was shown that they cannot be the ground state. We could not obtain the uncorrelated antiferromagnetic [111] configuration observed in $GeCo_2O_4$ and $GeNi_2O_4$ as the ground spin state, probably because we neglected two more parameters γ and J_4. We have obtained also cone-helices [110]-A and B, shown in Fig.9 or 10, respectively, which have the lowest energy among the configurations that we constructed with one wavevector or two wavevectors along [001], [110], and [111], in regions denoted by (h) and (i), respectively, in Figs.11 and 12. It was found, however,

that the eigenvalues of these cone-helices are higher than either the eigenvalue for q = $(\pi/2,\pi/4,0)$ or eigenvalues for q's in the vicinity of (k,0,k) and $(\pi/2,k,k)$, so that their stability has not been warranted. The observed low-temperature structure of $MgCr_2O_4$ seems to contain wavevectors $(\pi/2,\pi/4,0)$ and $(\pi/4,\pi/4,0)$ and that of $ZnFe_2O_4$ a wavevector $(\pi/2,\pi/4,0)$. It would therefore be interesting to construct such structures and study their stability in the regions in which the stability of the cone-helix [110]-A or B was not warranted with respect to $(\pi/2,\pi/4,0)$.

Appendix A: Construction of the (k,k,0) Spin Configurations in §4

First we determine k from $d\lambda_1^{[110]}(k)/dk = 0$, taking β as constant. We can choose β to satisfy one of following two equations:

$$X/Y = u_1/u_2 = 1,\ X' = Y' = 0,\ \text{i.e.,}\ u_1 = u_2 = u_3 = u_4, \tag{A-1}$$

$$X/Y = u_1/u_2 = -1,\ X' = Y' = 0,\ \text{i.e.,}\ u_1 = -u_2 = u_3 = -u_4. \tag{A-2}$$

From (A-1), we obtain the helix [110], denoted by (g), with following equations:

$$\beta^2 = \frac{C_{11}(k) + C_{24}(k) + 2C_{12}(k)}{C_{11}(k) + C_{13}(k) + 2C_{12}(k)}, \tag{A-3}$$

$$\lambda_1^{[110]}(k) = C_{11}(k) + C_{24}(k) + 2C_{12}(k). \tag{A-4}$$

The corresponding energy is

$$E/NS^2 = \lambda_1^{[110]}(k)(2 + 2/\beta^2). \tag{A-5}$$

This configuration has a lower energy in a region of $\xi < 0$ in the case of $\zeta = 1/2$ and $J_2 < 0$ (see Fig. 8), provided k is in the interval $(0, \pi/2)$.

From (A-2) we obtain another helix [110] for which k in the above is replaced by $\pi - k$, i.e., $C_{12}(k)$ by $-C_{12}(k)$, but the corresponding energy for k in the interval $(0, \pi/2)$ is found to be high in the shaded regions of Figs. 3, 4, 5.

Next we construct spin configurations with two wavevectors, $Q = (k,k,0)$ and $Q' = (\pi/2, \pi/2, 0)$ as follows:

(h) Cone-helix [110]-A

We force degeneracy of two eigenvalues $\lambda_1^{[110]}(k)$ and $\lambda_2^{[110]}(\pi/2)$. We then obtain β^2 as

$$\beta^2 = \frac{\{C_{11}(k) + C_{13}(k) - A(\pi/2)\}\{C_{11}(k) + C_{24}(k)\} - 4C_{12}(k)^2}{A(\pi/2)\{C_{11}(k) + C_{13}(k)\} - A(\pi/2)^2}, \tag{A-6}$$

where

$$A(\pi/2) = -2J_2(\xi - 2\eta + 2\zeta - 2). \tag{A-7}$$

From Eq. (4.2) we have

$$X/Y = u_1(k)/u_2(k) = -\frac{C_{11}(k) + C_{24}(k) - \lambda_2^{[110]}(\pi/2)}{2C_{12}(k)}, \tag{A-8}$$

and we must have

$$|u_1(k)/u_2(k)| \leq 1 \tag{A-9}$$

in order to satisfy (4.11). The corresponding energy is

$$E/NS^2 = \lambda_2^{[110]}(\pi/2)(2 + 2/\beta^2). \tag{A-10}$$

(i) Cone-helix [110]-B

We force degeneracy of two eigenvalues $\lambda_1^{[110]}(k)$ and $\lambda_3^{[110]}(\pi/2)$. Then we have

$$\beta^2 = \frac{\lambda_3^{[110]}(\pi/2)\{C_{11}(k) + C_{24}(k)\} - \lambda_3^{[110]}(\pi/2)^2}{\{C_{11}(k) + C_{13}(k)\}\{C_{11}(k) + C_{24}(k)\} - 4C_{12}(k)^2}, \tag{A-11}$$

$$X/Y = u_1(k)/u_2(k) = -\frac{C_{11}(k) + C_{24}(k) - \lambda_3^{[110]}(\pi/2)}{2C_{12}(k)}, \tag{A-12}$$

$$|u_1(k)/u_2(k)| \geq 1. \tag{A-13}$$

The corresponding energy is

$$E/NS^2 = \lambda_3^{[110]}(\pi/2)(2 + 2/\beta^2). \qquad \text{(A-14)}$$

Appendix B: Construction of the (k,k,k) Spin Configurations in §5

We first consider the configurations having one wavevector q = (k,k,k). From Eq. (5.3) we have the eigenvalue $\lambda_1^{[110]}(k)$ with u_1, $u_2 = u_3 = u_4$. We determine k from $d\lambda_1^{[111]}(k)/dk = 0$. We can choose β to satisfy

$$u_1/x = u_1/\sqrt{3}u_2 = 1/\sqrt{3}, \text{ i.e., } u_1 = u_2 = u_3 = u_4, \tag{B-1}$$

or

$$u_1/x = u_1/\sqrt{3}u_2 = -1/\sqrt{3}, \text{ i.e., } u_1 = -u_2 = -u_3 = -u_4. \tag{B-2}$$

From (B-1) we obtain a helix [111], with

$$\beta^2 = \frac{C_{11}(k) + C_{12}(k) + 2C_{23}(k)}{C_{11}(k) + 3C_{12}(k)}, \tag{B-3}$$

$$\lambda_1^{[111]}(k) = C_{11}(k) + C_{12}(k) + 2C_{23}(k). \tag{B-4}$$

The exchange energy is

$$E/NS^2 = \lambda_1^{[111]}(k)(3 + 1/\beta^2). \tag{B-5}$$

The helix [111] has a lower energy in the case of $\zeta = 1/2$ and $J_2 < 0$, as shown in Fig. 8.

From (B-2) we obtain another helix [111], with

$$\beta^2 = \frac{C_{11}(k) - C_{12}(k) + 2C_{23}(k)}{C_{11}(k) - 3C_{12}(k)}, \tag{B-6}$$

$$\lambda_1^{[111]}(k) = C_{11}(k) - C_{12}(k) + 2C_{23}(k). \tag{B-7}$$

The change of sign of $C_{12}(k)$, as compared with the former case, means that k has been replaced by $\frac{\pi}{2} - k$. Here $C_{12}(k)$ must be positive in order that this eigenvalue is lower than that given by Eq. (B-4). But the corresponding energy is found to be very high in the shaded regions of Figs. 3,4,5.

Next we construct configurations having two wavevectors Q = 0 and Q' = $(\pi/4, \pi/4, \pi/4)$ and obtain a Yafet-Kittel-like [111] configuration by forcing degeneracy of two eigenvalues $\lambda_1^{[111]}(0)$ and $\lambda_x^{[111]}(\pi/4)$, with

$$\beta^2 = \frac{\lambda_x^{[111]}(\pi/4)(C_{11}(0) + 2C_{12}(0)) - \lambda_x^{[111]}(\pi/4)^2}{C_{11}(0)(C_{11}(0) + 2C_{12}(0) - \lambda_x^{[111]}(\pi/4)) - 3C_{12}(0)^2} . \qquad \text{(B-8)}$$

From Eq. (5.2) we have

$$x/\sqrt{3}u_1 = u_2(0)/u_1(0) = - \frac{\sqrt{3}C_{12}(0)}{C_{11}(0) + 2C_{12}(0) - \lambda_1^{[111]}(\pi/4)}, \qquad \text{(B-9)}$$

and from the condition (5.7) we require

$$|u_2(0)/u_1(0)| \leq 1. \qquad \text{(B-10)}$$

Appendix C: Effects of γ and J_4

If we take γ and J_4 into account, we have additional terms

$$\begin{aligned} & 2J_2\gamma[\cos 2(q_x + q_y) + \cos 2(q_y + q_z) + \cos 2(q_z + q_x) \\ & \quad -\cos 2(q_x - q_y) - \cos 2(q_y - q_z) - \cos 2(q_z - q_x)] \\ & \quad - 2J_4(\cos 4q_x + \cos 4q_y + \cos 4q_z) \end{aligned} \tag{C-1}$$

to $C_{11}(q_x,q_y,q_z)$. Other diagonal elements are related to this by equations.

$$C_{22}(q_x,q_y,q_z) = C_{11}(-q_x,q_y,q_z), \tag{C-2}$$

$$C_{33}(q_x,q_y,q_z) = C_{11}(q_x,q_y,-q_z), \tag{C-3}$$

$$C_{44}(q_x,q_y,q_z) = C_{11}(q_x,-q_y,q_z). \tag{C-4}$$

The off-diagonal elements do not contain γ and J_4.

(1) The case of $q = (0,0,k)$

The matrix elements have the symmetry $C_{11}(k) = C_{22}(k) = C_{33}(k) = C_{44}(k)$, $C_{12}(k) = C_{14}(k) = C_{23}(k) = C_{34}(k)$, $C_{13}(k) = C_{24}(k)$. Thus, we can use transformation (3.1) and obtain four eigenvalues, of which the degenerate eigenvalues for X_2 and X_4 are

$$\lambda_2^{[001]}(k) = \lambda_4^{[001]}(k) = C_{11}(k) - C_{13}(k), \tag{C-5}$$

with $u_1 = -u_3$, $u_2 = -u_4$. The UA2 configuration has the eigenvalue

$$\lambda_2^{[001]}(\pi/2) = \lambda_4^{[001]}(\pi/2) = -2J_2(-\xi + 2\eta - 2\zeta - 2) - 6J_4. \tag{C-6}$$

(2) The case of $q = (k,k,k)$

The matrix $[C_{\mu\nu}(k)]$ has the symmetry $C_{11}(k) \neq C_{22}(k) = C_{33}(k) = C_{44}(k)$, $C_{12}(k) = C_{13}(k) = C_{14}(k)$, $C_{23}(k) = C_{24}(k) = C_{34}(k)$. Thus, we can use transformation (5.1) and obtain the following eigenvalue equation for u_1 and x:

$$\begin{vmatrix} C_{11}(k) - \lambda/\beta^2 & \sqrt{3}C_{12}(k) \\ \sqrt{3}C_{12}(k) & C_{22}(k) + 2C_{23}(k) - \lambda \end{vmatrix} = 0. \qquad \text{(C-7)}$$

When k is equal to $\pi/4$, we have $C_{12}(\pi/4) = 0$, and hence we have two eigenvalues

$$\lambda^{[111]}(\pi/4) = -6\beta^2(2J_2\gamma - J_4), \qquad \text{(C-8)}$$

$$\lambda_x^{[111]}(\pi/4) = -4J_2(\xi - 2\zeta - \gamma) + 6J_4, \qquad \text{(C-9)}$$

with $u_1 \neq 0$, $u_2 = u_3 = u_4 = 0$ and $u_1 = 0$, $u_2 = u_3 = u_4 \neq 0$, respectively.

References

1) F. K. Lotgering: Proc. Intern. Conf. on Magnetism, Nottingham 533 (1964); Solid State Communications 3, 347 (1965).

2) R. Plumier: Comt. Rend. 260, 3348 (1965); J. Appl. Phys. 37, 964 (1966).

3) P. K. Baltzer, H. W. Lehmann, and M. Robbins: Phys. Rev. Letters 15, 493 (1965); N. Menyuk, K. Dwight, R. J. Arnott, and A. Wold: J. Appl. Phys. 37, 1387 (1966); R. C. LeCraw, H. Von Philipsborn, and M. D. Sturge: J. Appl. Phys. 38, 965 (1967).

4) P. K. Baltzer, P. J. Wojtowicz, M. Robbins, and E. Lopatin: Phys. Rev. 151, 367 (1966).

5) J. M. Hastings and L. M. Corliss: J. Phys. Chem. Solids 29, 9 (1968).

6) K. Dwight and N. Menyuk: Phys. Rev. 163, 435 (1967).

7) D. H. Lyons and T. A. Kaplan: Phys. Rev. 120, 1580 (1960).

8) J. M. Hastings and L. M. Corliss: Phys. Rev. 102, 1460 (1956).

9) E. F. Bertaut et al.: Proc. Intern, Conf. on Magnetism, Nottingham 275 (1964).

10) E. F. Bertaut et al.: J. Phys. Radium 25, 516 (1964).

11) R. Plumier and A. Tardieu: Compt. Rend. 257, 3858 (1963).

12) R. Plumier: Compt. Rend. 267, 98 (1968); R. Plumier and M. Sougi: Compt. Rend. 268, 365 (1969).

13) H. Shaked, J. M. Hastings, and L. M. Corliss: Phys. Rev. B1, 3116 (1970).

14) T. Nagamiya: Solid State Physics Vol. 20, Seitz and Turnbull ed. (1967); J. Appl. Phys. 39, 373 (1968).

15) D. H. Lyons, T. A. Kaplan, K. Dwight, and N. Menyuk: Phys. Rev. 126, 540 (1962).

16) Y. Aiyama: J. Phys. Soc. Japan 21, 1684 (1966).

17) A. Oleś et al.: Tables of Magnetic Structures Determined by Neutron Diffraction, Part I-Cubic System, 77 (1970).

Table I. Difference in notation used for the interaction constants due to various investigators.

Interaction*	Distance	Present paper	DM[6]	BWRL[4]	LP[1), 2)]
B-O-B	$\sqrt{2}\frac{a}{4}$	$J_0 = \xi J_2$	J	J	W_0
B-O-O-B	$\sqrt{6}\frac{a}{4}$	$J_1 = \eta J_2$	WJ	K	W_1
B-O-O-B	$\sqrt{8}\frac{a}{4}$	$J_2' = (1 - \gamma)J_2$	UJ = UJ(1 - γ)	.....	W_2
B-O-O-B (A′)	$\sqrt{8}\frac{a}{4}$	$J_2'' = (1 + \gamma)J_2$	U'J = UJ(1 + γ)	K	W_2
B-O-O-B (A′)	$\sqrt{10}\frac{a}{4}$	$J_3 = \zeta J_2$	VJ	K	.....
B-O-O-O-B	$\sqrt{16}\frac{a}{4}$	J_4	U_2J	.....	.....

*B: magnetic cation in B-site

O: anion

A: nonmagnetic cation in A-site

Fig. 1. Positions of anions (open circles), nonmagnetic cations in A-sites (hatched circles), and magnetic cations in B-sites (black circles) in a part of the spinel lattice. The paths of six superexchange interactions are as follows:

J_0: 1-c-3; 1-d-3.

J_1: 1-a $\overset{A}{-}$ j-2'; 1-d-j-2'; 1-d $\overset{A}{-}$ e-2'; 1-d-k-2'; 1-i-j-2'.

J_2': 1-c-f-1'; 1-d-g-1'.

J_2'': 1-a $\overset{A}{-}$ b-1''; 1-d $\overset{A}{-}$ e-1''.

J_3: 1-d $\overset{A}{-}$ e-3'.

J_4: 1-d $\overset{A}{-}$ e-h-1'''; 1-d-g $\overset{A}{-}$ h-1'''.

Fig. 2. Uncorrelated antiferromagnetic [001] configuration-2. The axis of (1, 3) and that of (2, 4) are not correlated.

Fig. 3. Regions of the [001] spin configurations in the $\xi\eta$ plane, in the case of $\zeta = 1/2$. Here $\xi = J_0/J_2$, $\eta = J_1/J_2$, $\zeta = J_3/J_2$. The boundaries of their stability regions are represented by bold lines. The ferromagnetic configuration is denoted by (a), helix [001]-1 by (b), helix [001]-2 by (c), degenerate antiferromagnetic configuration by (d), and uncorrelated antiferromagnetic [001] configuration-2 by (f). Straight lines (e) for $J_2 > 0$ and for $J_2 < 0$ represent the uncorrelated antiferromagnetic [001] configuration-1. Bold lines and dashed lines in the (b) and (c) regions denote curves of constant Q = (0,0,k). Shaded regions are unstable regions.

Fig. 4. The case of $\zeta = 0$, similar to Fig. 3.

Fig. 5. The case of $\zeta = -1/2$, similar to Fig. 3.

Fig. 6. The eighth of the first Brillouin zone. The forty-eighth of the zone for the [001] configurations is shown by bold lines. The stability of the [001] configurations is investigated with respect to a number of q vectors, in particular those along [110], [111], and [210], and special

q vectors at 19 points on the zone face marked by x and 3 points within the zone marked by ●. The sixteenth of the first Brillouin zone for the [110] configurations in §4 is represented by chain lines. The part of $q_z > 0$ of the twelfth of the first Brillouin zone for the [111] configurations in §5 is shown by bold and fine lines.

Fig. 7. Observed correlated antiferromagnetic [001] configuration in MgV_2O_4.

Fig. 8. Regions of lower energy for helix [110], helix [111], and cone-helices [110]-A and B in the case of $\zeta = 1/2$ and $J_2 < 0$. Their boundaries are marked by chain lines.

Fig. 9. Cone-helix [110]-A ($0 < u_1(k)/u_2(k) < 1$)

Fig. 10. Cone-helix [110]-B ($u_1(k)/u_2(k) < -1$)

Fig. 11. Regions of lower energy for cone-helices [110]-A and B in the case of $\zeta \neq 0$. The boundaries of their regions are shown by chain lines. Dashed lines denote curves of $k = 3\pi/8$. As regards the Yafet-Kittel-like [111] configuration, see §5.

Fig. 12. Regions of lower energy for cone-helices [110]-A and B in the case of $\zeta = 0$, similar to Fig. 11.

Fig. 13. Bad wavevectors on the plane $q_x = \pi/2$ in the zone for the cone-helix [110]-B, in the case of $\zeta = 0$ and $J_2 > 0$. Bad wavevectors are represented by x for the case of $\xi = -6.0$ and $\eta = 2.0$ and by ⊗ for both of $\xi = -6.0$, $\eta = 2.0$ and $\xi = -6.0$, $\eta = 3.5$.

Fig. 14. Yafet-Kittle-like [111] configuration.

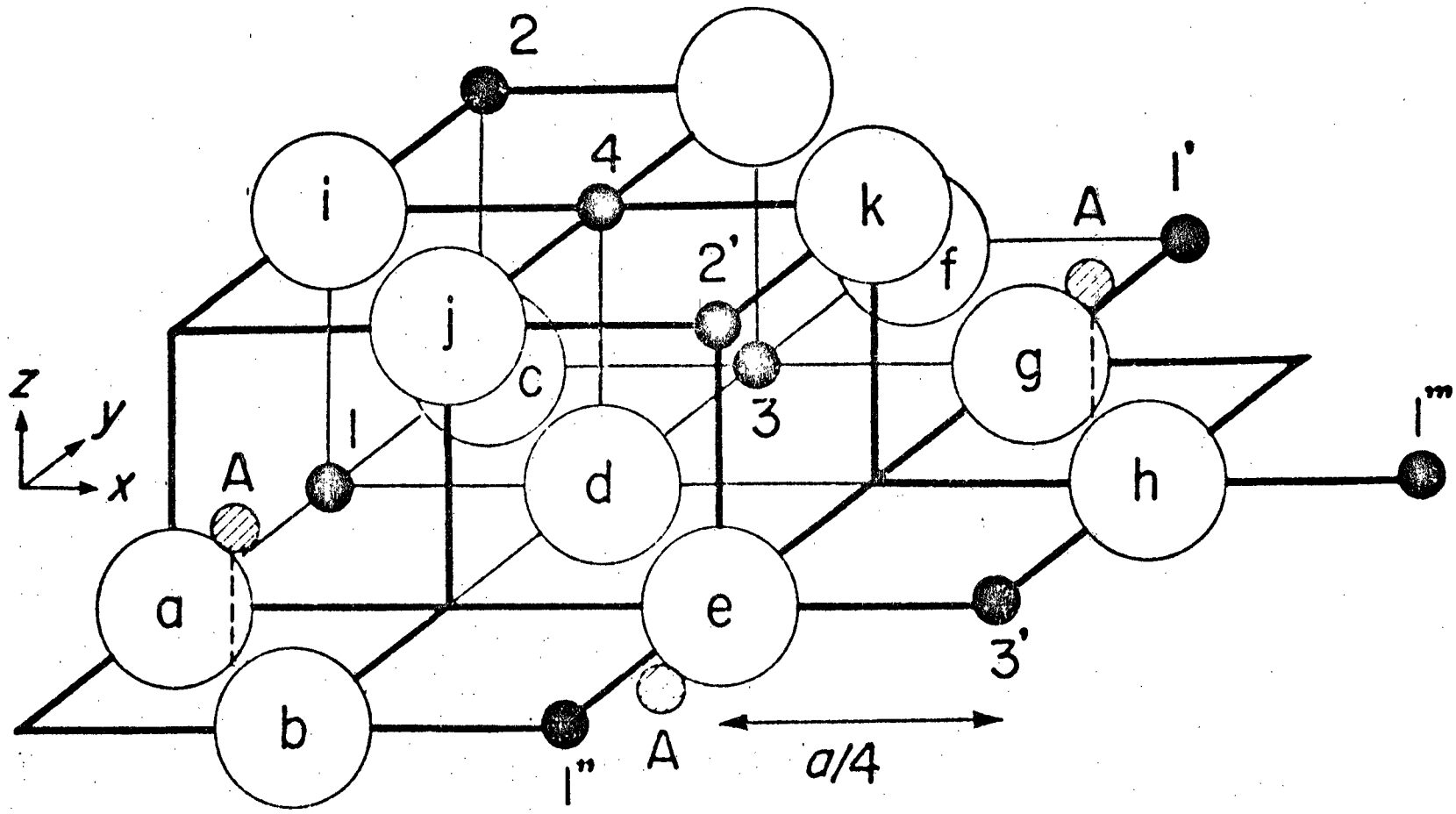

Fig. 1

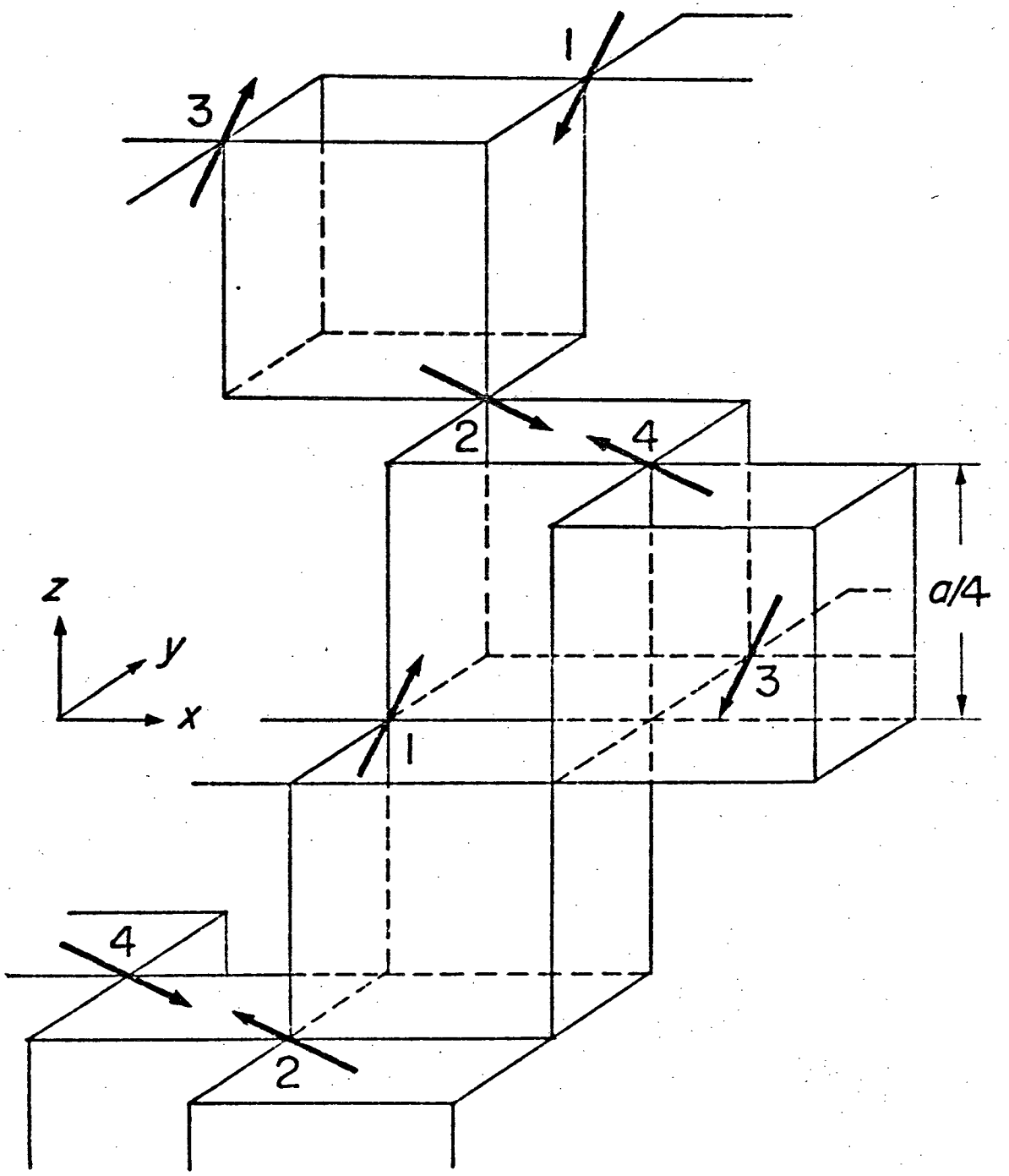

Fig. 2

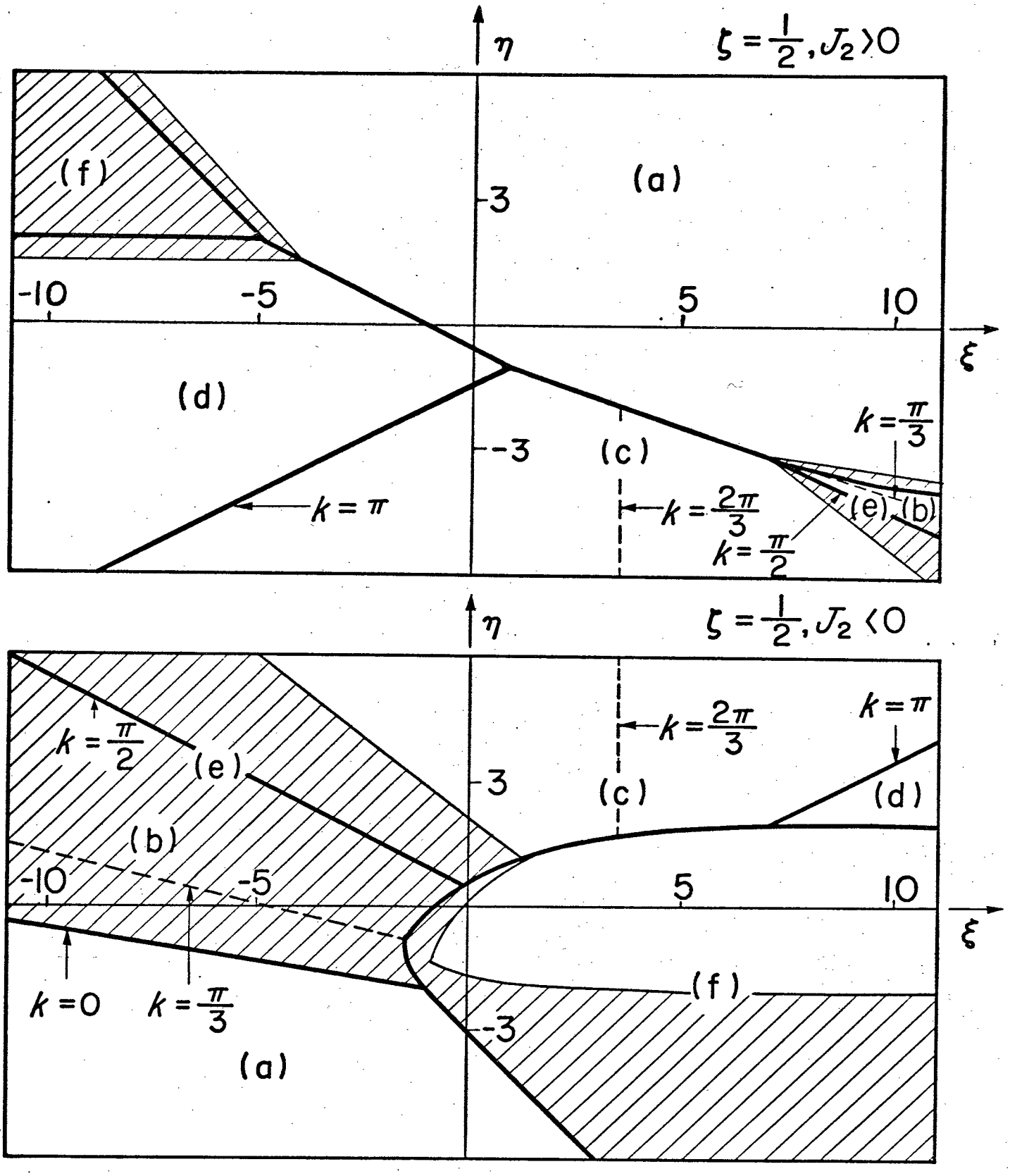
η
ζ = 1/2, J2 > 0
(f)
(a)
3
-10
-5
5
10
ξ
(d)
k = π/3
-3
(c)
k = π
k = 2π/3
(e)
(b)
k = π/2
η
ζ = 1/2, J2 < 0
k = π/2
(e)
k = 2π/3
k = π
3
(c)
(d)
(b)
-10
-5
5
10
ξ
k = 0
k = π/3
(f)
-3
(a)

Fig. 3

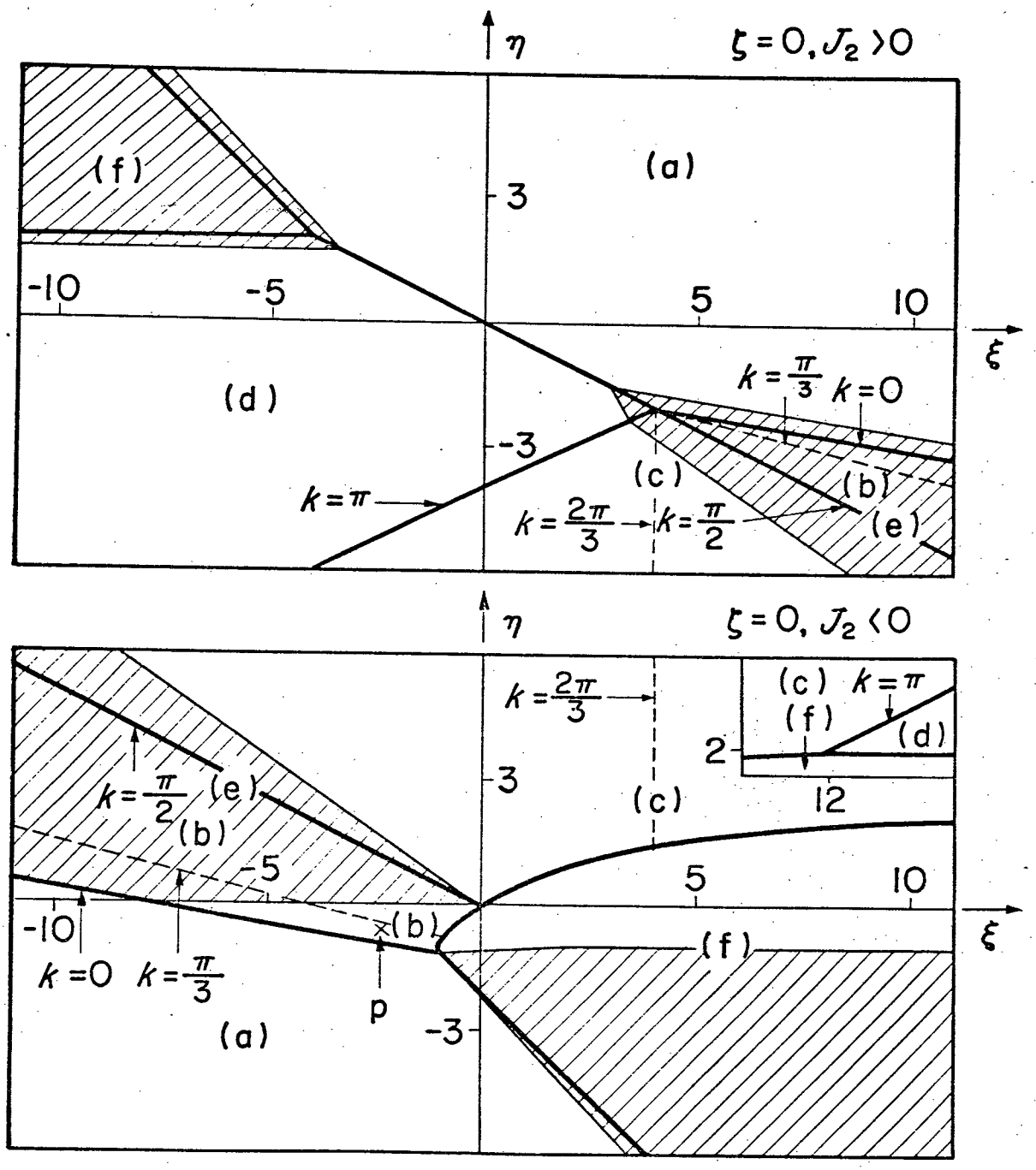
η
ζ = 0, J₂ > 0
(f)
(a)
3
-10
-5
5
10
ξ
(d)
k = π/3
k = 0
-3
(c)
(b)
k = π
k = 2π/3
k = π/2
(e)
η
ζ = 0, J₂ < 0
k = 2π/3
(c)
k = π
(f)
(d)
2
12
3
k = π/2
(e)
(b)
-5
5
10
-10
(b)
(f)
k = 0
k = π/3
p
(a)
-3
ξ

Fig. 4

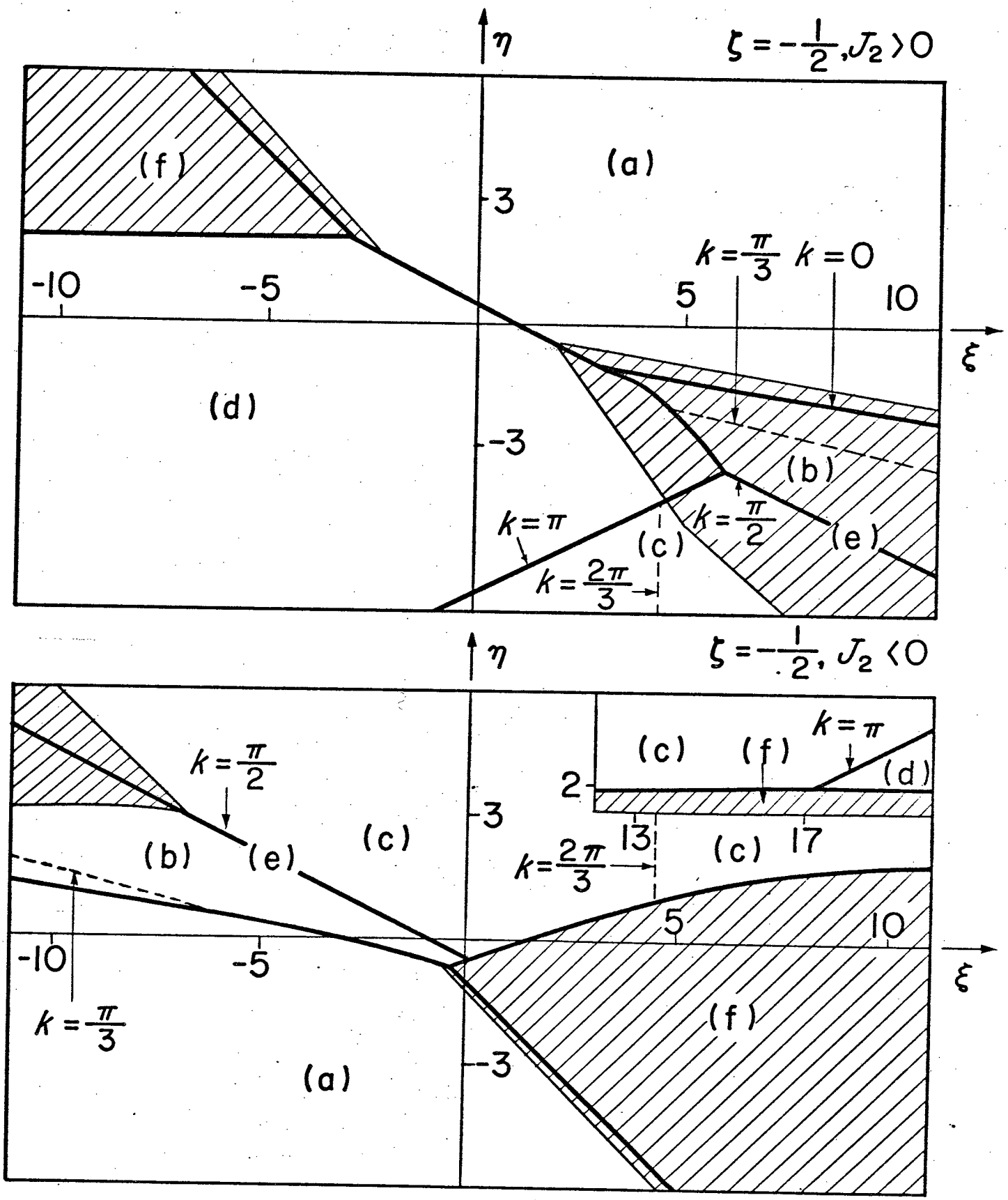
η
ζ = -1/2, J2 > 0
(a)
(b)
(c)
(d)
(e)
(f)
3
-3
-10
-5
5
10
ξ
k = π/3
k = 0
k = π/2
k = π
k = 2π/3
η
ζ = -1/2, J2 < 0
(a)
(b)
(c)
(d)
(e)
(f)
3
-3
2
13
17
-10
-5
5
10
ξ
k = π/3
k = π/2
k = π
k = 2π/3

Fig. 5

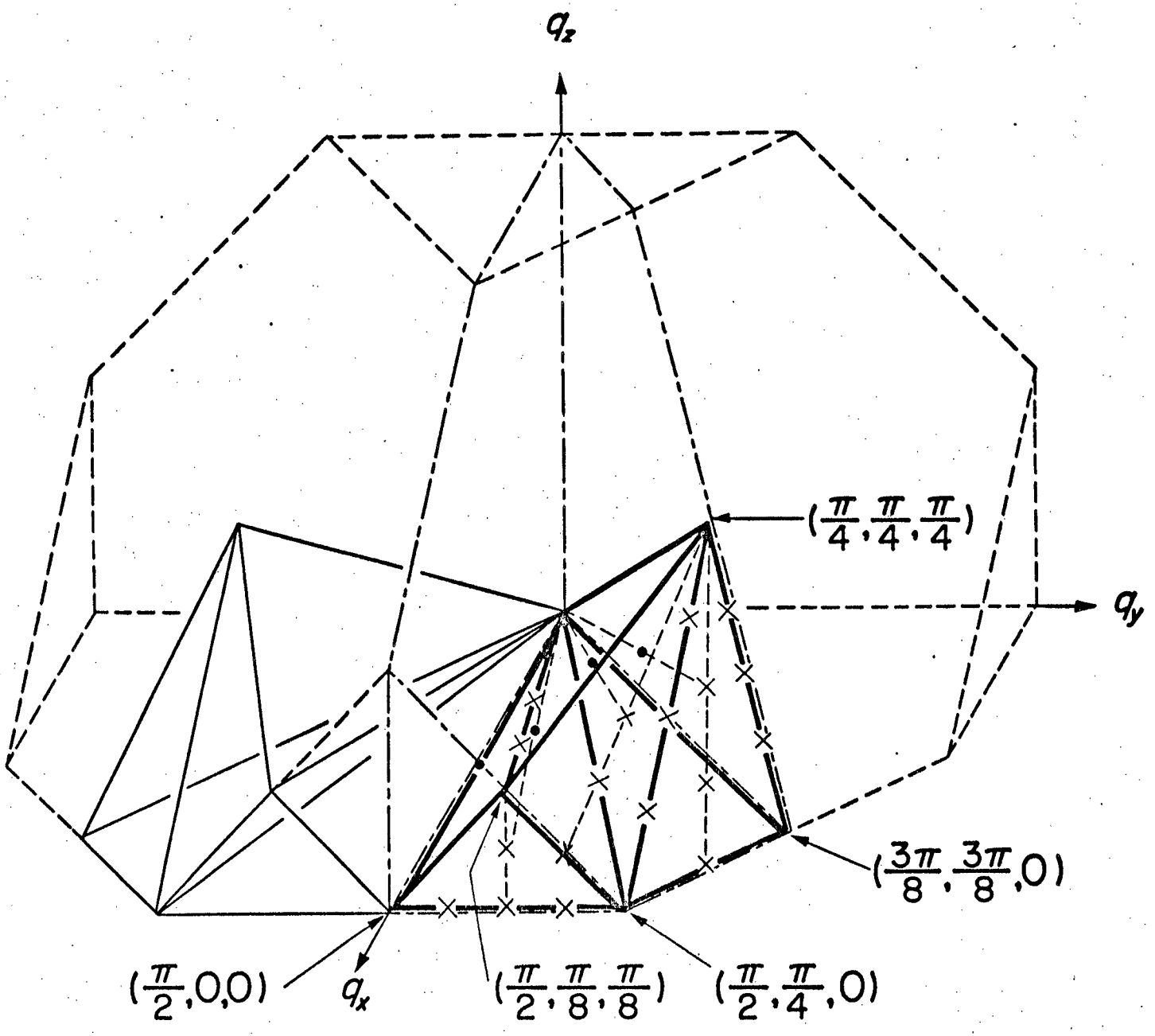
q_z
q_y
q_x
$(\frac{\pi}{4},\frac{\pi}{4},\frac{\pi}{4})$
$(\frac{3\pi}{8},\frac{3\pi}{8},0)$
$(\frac{\pi}{2},0,0)$
$(\frac{\pi}{2},\frac{\pi}{8},\frac{\pi}{8})$
$(\frac{\pi}{2},\frac{\pi}{4},0)$

Fig. 6

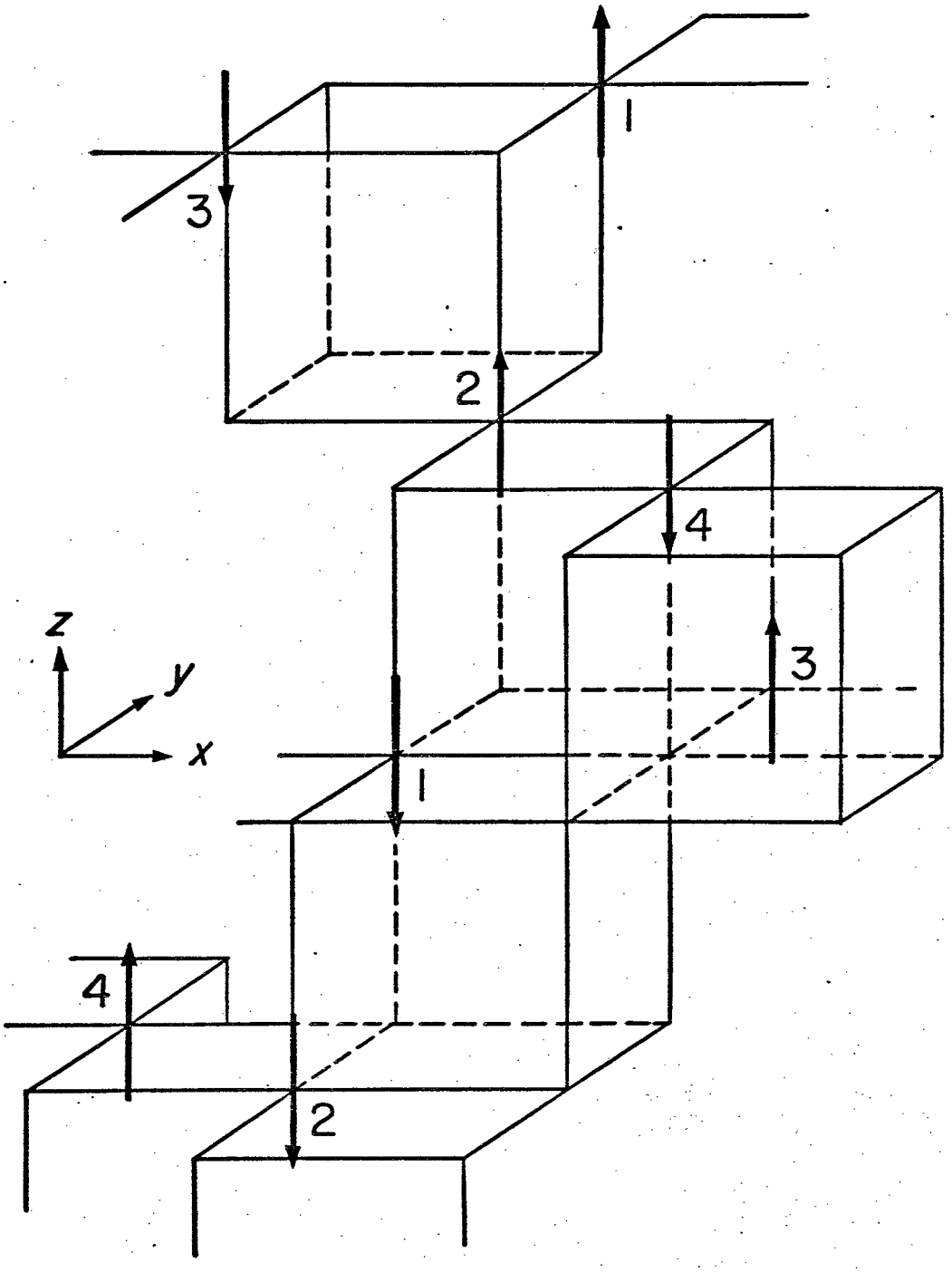

Fig. 7

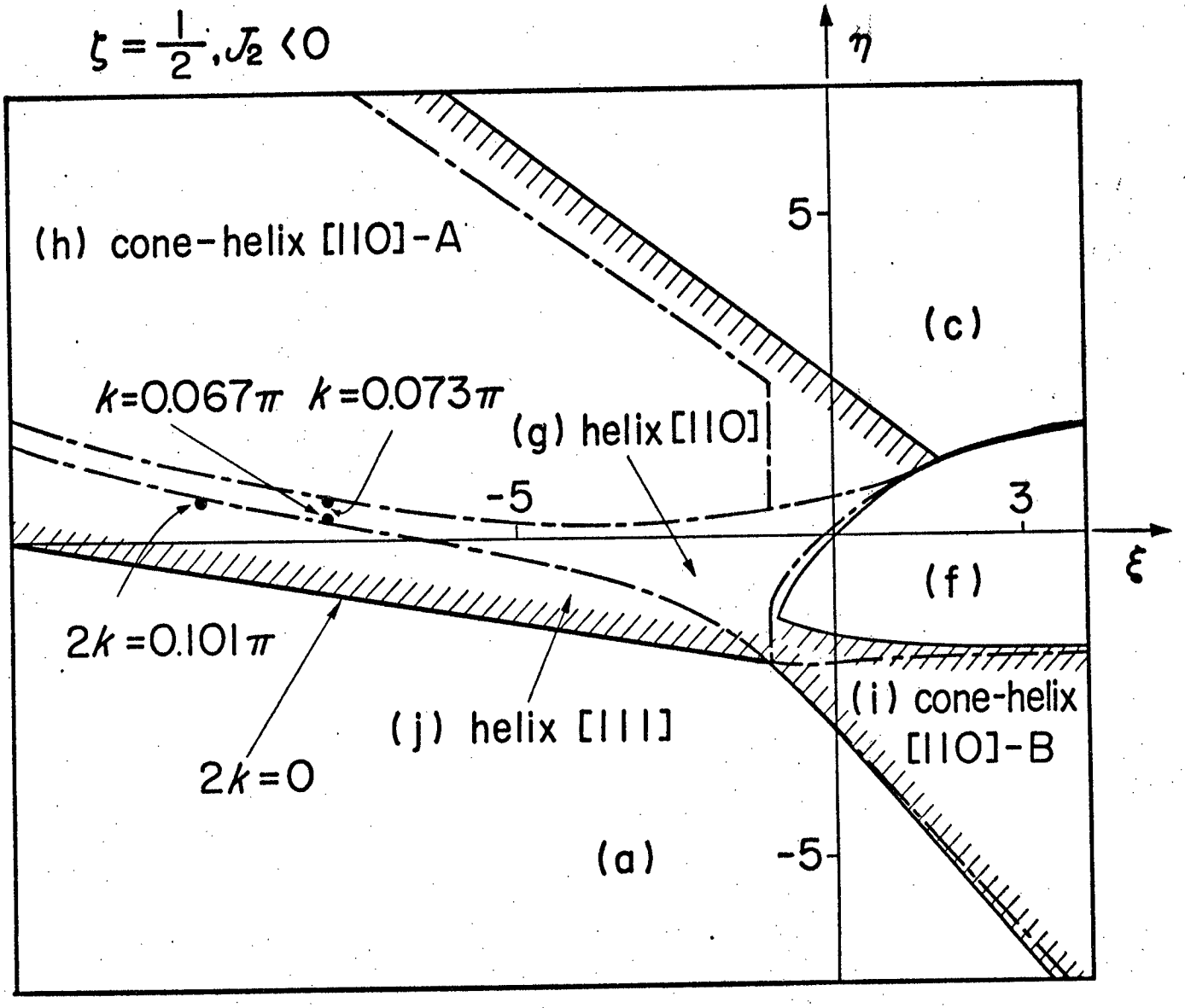
ζ = 1/2, J2 < 0
η
5
(h) cone-helix [110]-A
(c)
k=0.067π
k=0.073π
(g) helix [110]
-5
3
ξ
(f)
2k=0.101π
(i) cone-helix
[110]-B
(j) helix [111]
2k=0
(a)
-5

Fig. 8

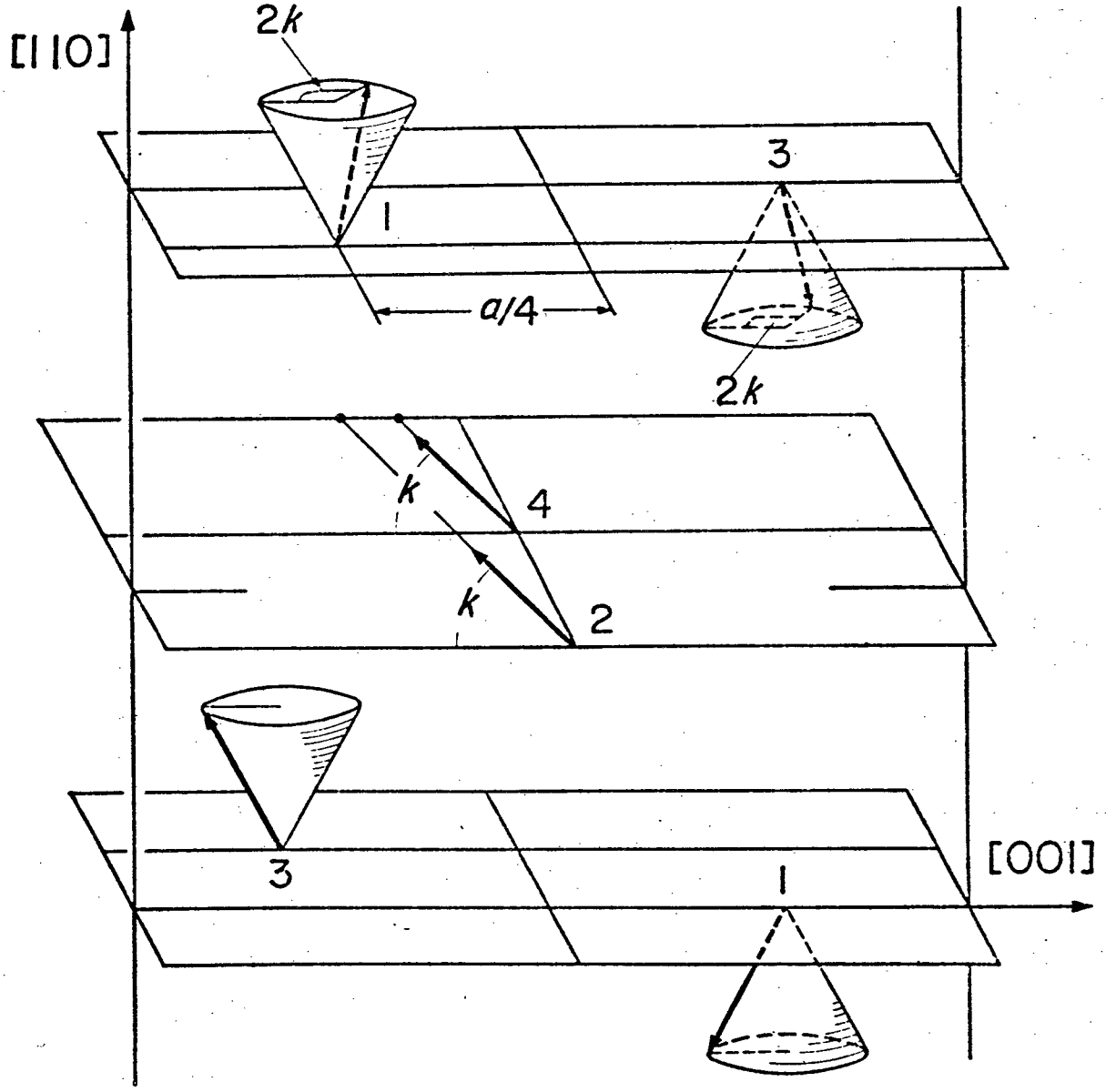

Fig. 9

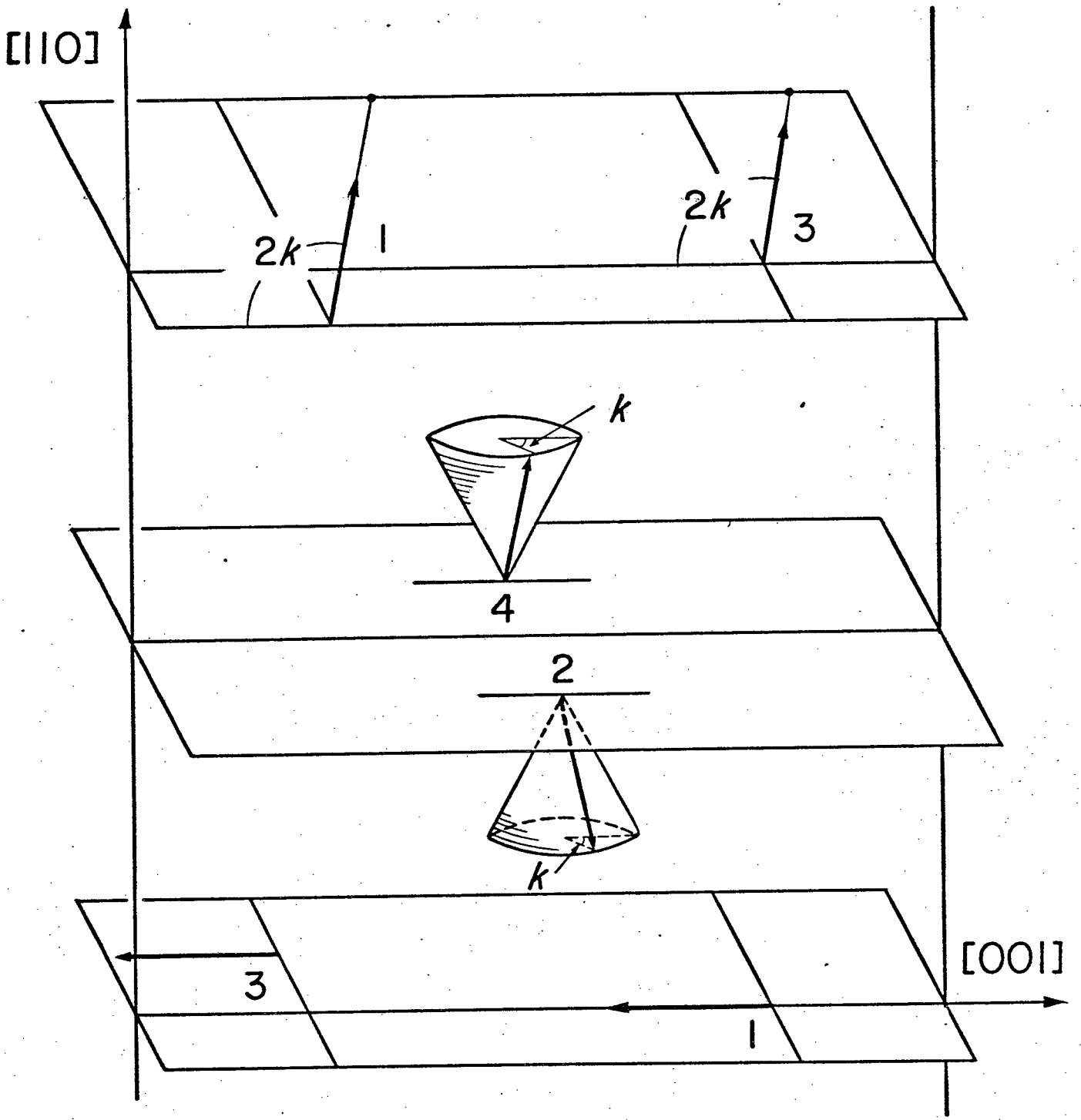

Fig. 10

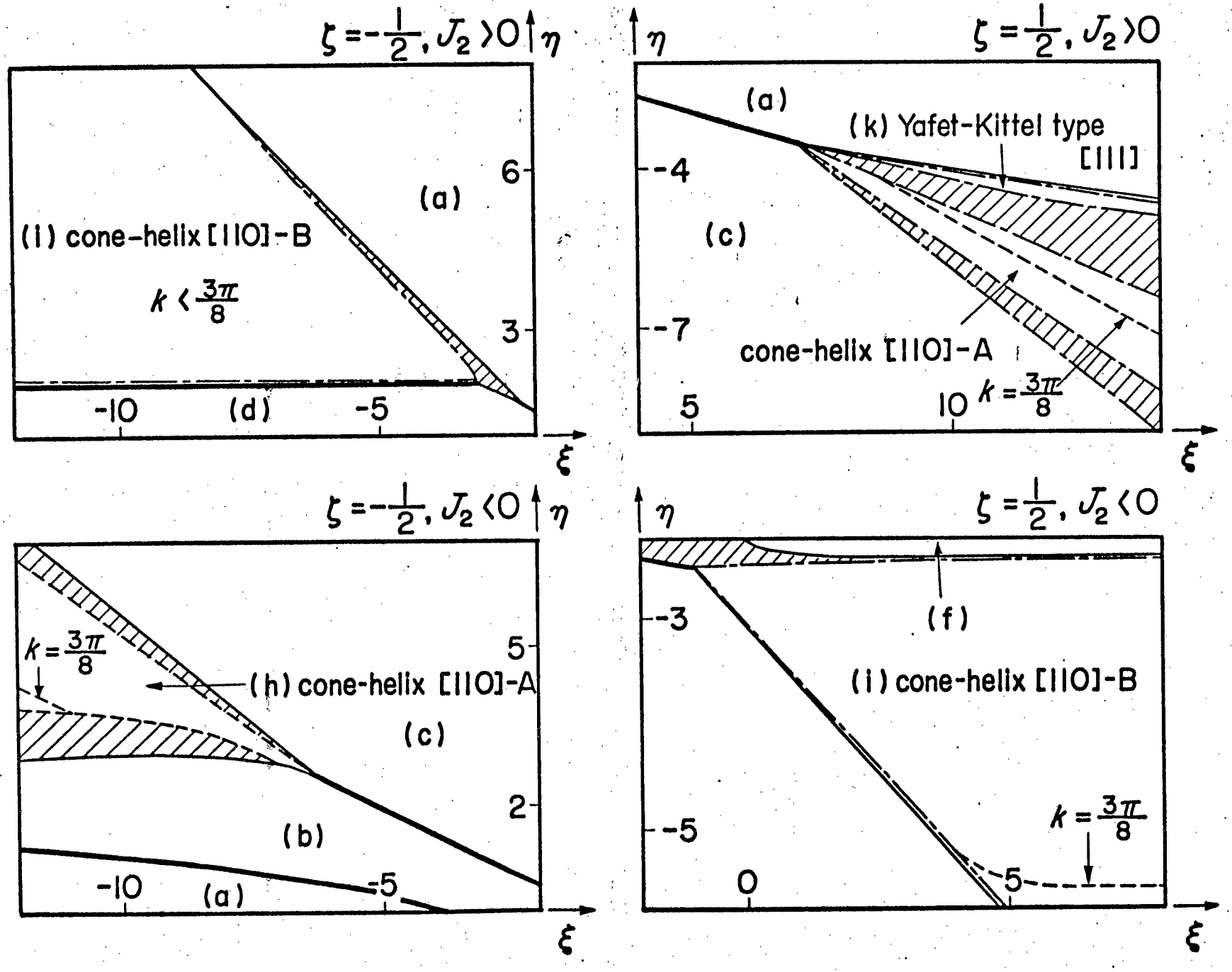
$\zeta = -\frac{1}{2}, J_2 > 0$
η
(a)
(l) cone-helix [110]-B
$k < \frac{3\pi}{8}$
6
3
-10
(d)
-5
ξ
$\zeta = \frac{1}{2}, J_2 > 0$
η
(a)
(k) Yafet-Kittel type
[111]
-4
(c)
-7
cone-helix [110]-A
5
10
$k = \frac{3\pi}{8}$
ξ
$\zeta = -\frac{1}{2}, J_2 < 0$
η
$k = \frac{3\pi}{8}$
(h) cone-helix [110]-A
(c)
5
2
(b)
-10
(a)
-5
ξ
$\zeta = \frac{1}{2}, J_2 < 0$
η
(f)
-3
(l) cone-helix [110]-B
-5
$k = \frac{3\pi}{8}$
0
-5
ξ

Fig. 11

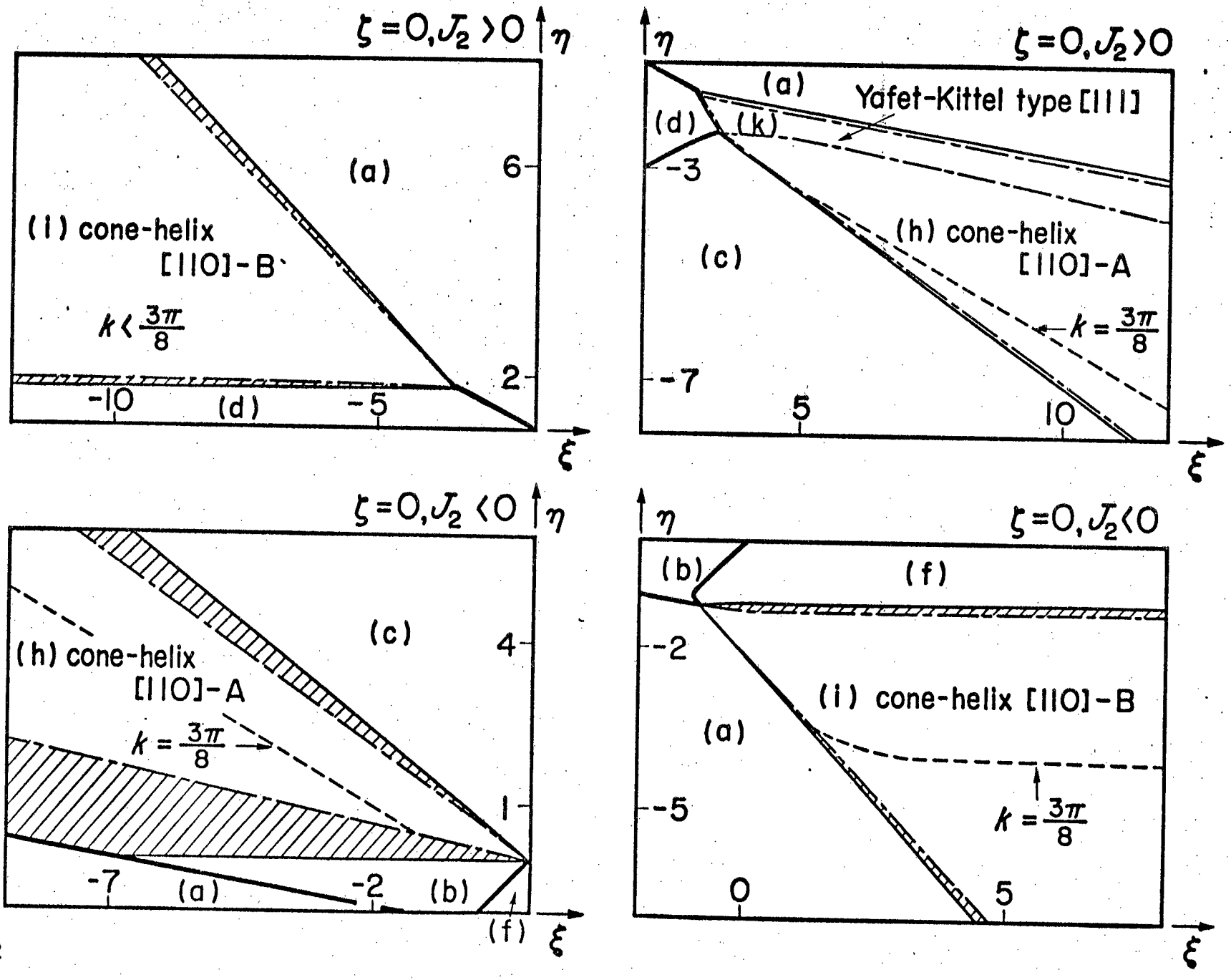
ζ=0, J₂>0
η
ξ
(a)
6
2
(l) cone-helix
[110]-B
k < 3π/8
-10
(d)
-5
ζ=0, J₂>0
η
ξ
(a)
Yafet-Kittel type [111]
(d)
(k)
-3
(h) cone-helix
[110]-A
(c)
k = 3π/8
-7
5
10
ζ=0, J₂<0
η
ξ
(c)
4
1
(h) cone-helix
[110]-A
k = 3π/8
-7
(a)
-2
(b)
(f)
ζ=0, J₂<0
η
ξ
(b)
(f)
-2
(l) cone-helix [110]-B
(a)
k = 3π/8
-5
0
5

Fig. 12

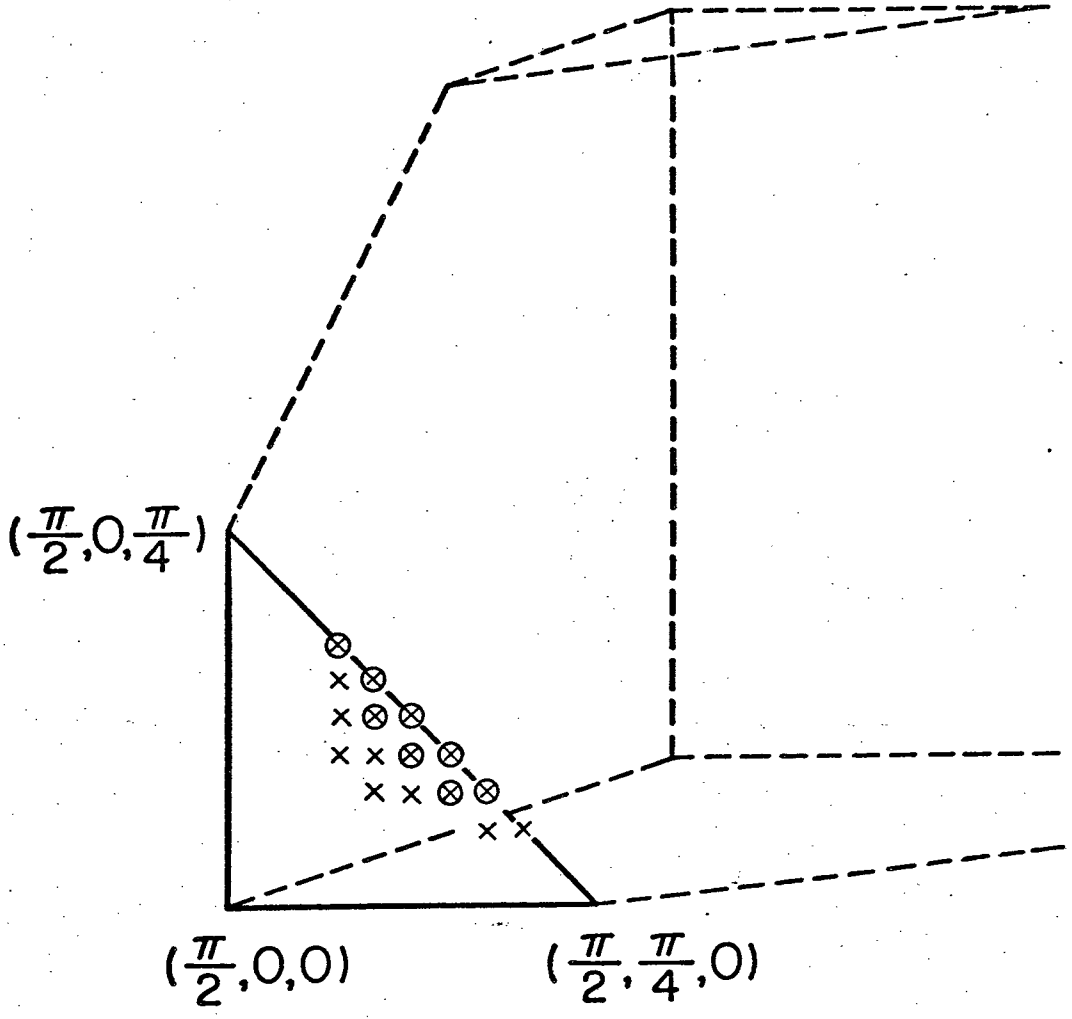

Fig. 13

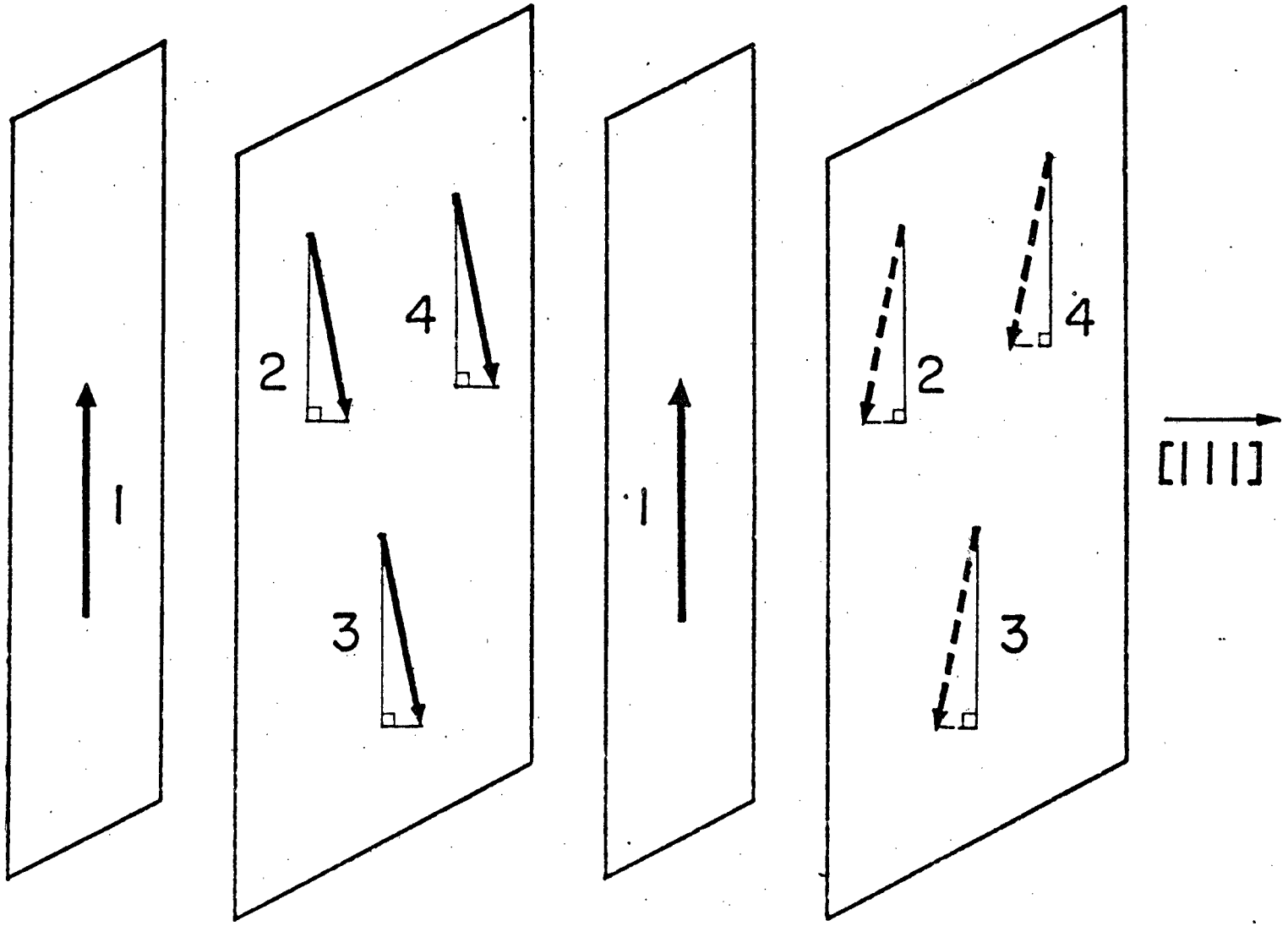

Fig. 14

Part II

Theory of Magnetic Structure of Zinc Ferrite

§1. Introduction

The spin structure of the normal cubic spinel $ZnFe_2O_4$ was first studied by Hastings and Corliss[1] by neutron diffraction at 2.7K using powder sample. A complicated pattern was observed whose dominant peaks corresponded to a wavevector $Q = (\pi/2,0,\pi/4)$ (measured in units of $4/a$, where a is the lattice constant) but the structure was not determined due to lack of resolution. A recent experiment by König et al.,[2] also using powder sample, showed well-resolved magnetic peaks up to high diffraction angles, and these peaks again corresponded to $Q = (\pi/2, 0, \pi/4)$ and could be indexed with a tetragonal magnetic unit cell of $a = b = 8.43\text{Å}$ and $c = 16.86\text{Å}$. Two possible models were proposed for the spin structure, one being a collinear spin configuration and the other a noncollinear spin configuration.

In Part I (quoted as I) we have theoretically studied possible ground spin configurations at $T = 0$ in the normal cubic spinel having magnetic cations on B-sites only. On the assumption of four different superexchange interactions we constructed spin configurations having one wavevector or two wavevectors restricted along [001], [110], and [111] and we studied their stability with respect to all wavevectors in whole Brillouin zone. It was shown among others that cone-helix [110]-A (see Fig. 9 in I) with two wavevectors (k,k,0) and $(0,0,\pi/2)$ has the lowest energy among all the constructed spin configurations in a certain region of the exchange-parameter space but that this configuration is unstable with respect to a wavevector $(\pi/2,0,\pi/4)$ in a certain part of that region. The same situation was found for cone-helix [110]-B (Fig. 10 in I). In Part II we therefore construct spin configurations with a wavevector $(\pi/2, 0,\pi/4)$ and study their stability. We extend our previous treatment in §2 and find new degenerate antiferromagnetic configurations. In §3 we study the effect of magnetic dipole-dipole interaction stabilizing particular ones of these antiferromagnetic configurations. In §4 we show that our results can be compared favorably with the spin structure observed for $ZnFe_2O_4$.

§2. Spin Configuration with a Wavevector $(\pi/2,0,\pi/4)$

We choose a rhombohedral unit cell containing four B-sites which are at 1. $(-1/2,-1/2,-1/2)$, 2. $(-1/2,1/2,1/2)$, 3. $(1/2,1/2,-1/2)$, 4. $(1/2,-1/2,1/2)$ in cubic coordinates measured in units of a/4. The exchange energy is written as

$$E_{ex}/NS^2 = \Sigma_q \Sigma_{\mu,\nu} C_{\mu\nu}(q)\sigma_{q\mu}\cdot\sigma_{q\nu}^{*}, \tag{2.1}$$

where $\sigma_{q\nu}$ and $C_{\mu\nu}(q)$, given by eqs. (2.3) and (2.2) of I, are respectively the Fourier transform of the classical spin vector $S_{n\nu}$ (of magnitude S, at the νth site in the nth unit cell) and the Fourier transform of the exchange constants $J(R_{m\mu} - R_{n\nu})$ ($R_{n\nu}$ being the position of $S_{n\nu}$), and N is the number of unit cells. We measure q in units of 4/a. We consider exchange interactions of four kinds: J_0 between nearest neighbors J_1 between second neighbors J_2' and J_2'' between third neighbors and J_3 between fourth neighbors (see Fig. 1 in I, where J_4 was also included). We write $J_2' = J_2(1 - \gamma)$ and $J_2'' = J_2(1 + \gamma)$, where γ is a measure of the degree of covalency of the A-site cation which lies on the superexchange path. Further, we write $\xi = J_0/J_2$, $\eta = J_1/J_2$, and $\zeta = J_3/J_2$.

The explicit form of the matrix $[C_{\mu\nu}(q_x,q_y,q_z)]$ was given in I. For $q = (2k,0,k)$ we have following expressions for $C_{\mu\nu}(2k,0,k)$, abbreviated as $C_{\mu\nu}(k)$:

$$C_{11}(k) = C_{44}(k) = -2J_2[\cos 6k + 2\cos 4k + 3\cos 2k - \gamma(\cos 6k - \cos 2k)], \tag{2.2a}$$

$$C_{22}(k) = C_{33}(k) = -2J_2[\cos 6k + 2\cos 4k + 3\cos 2k + \gamma(\cos 6k - \cos 2k)], \tag{2.2b}$$

$$C_{12}(k) = C_{34}(k) = -2J_2[\xi\cos k + \eta(\cos 5k + \cos 3k) + \zeta(\cos 3k + \cos k)], \tag{2.2c}$$

$$C_{13}(k) = C_{24}(k) = -2J_2[\xi\cos 2k + \eta(\cos 4k + 1) + \zeta(\cos 6k + \cos 2k)], \tag{2.2d}$$

$$C_{14}(k) = -2J_2[\xi\cos 3k + 2\eta\cos k + \zeta(\cos 5k + \cos k)], \tag{2.2e}$$

$$C_{23}(k) = -2J_2[\xi\cos k + 2\eta\cos 3k + \zeta(\cos 7k + \cos 5k)], \tag{2.2f}$$

We shall confine ourselves to $k = \pi/4$, i.e., to $Q = (\pi/2,0,\pi/4)$ which is one of K/4's, a quarter of a reciprocal lattice vector. Then, we have relations

$C_{11}(\pi/4) = C_{22}(\pi/4) = C_{33}(\pi/4) = C_{44}(\pi/4) = 4J_2$, $C_{12}(\pi/4) = C_{23}(\pi/4) = C_{34}(\pi/4) = -C_{14}(\pi/4) = -2J_2(\xi - 2\eta)$, $C_{13}(\pi/4) = C_{24}(\pi/4) = 0$. We denote by ε_Q the exchange energy terms of (2.1) with $q = Q$ and $q = -Q$:

$$\varepsilon_Q = \Sigma_{\mu,\nu} C_{\mu\nu}(\pi/4)\sigma_\mu \cdot \sigma_\nu^* + c.c., \tag{2.3}$$

and minimize (2.3) under the condition $S_{n\nu}^2 = S^2$ for all n and ν, which can be written as

$$[\sigma_\nu \exp(iQ \cdot R_{n\nu}) + c.c.]^2 = 1 \quad \text{for all n and } \nu. \tag{2.4}$$

$R_{n\nu} = R_n + R_\nu$, where R_n is a lattice translation vector and R_ν the position of one of the four B-sites, and for convenience we use $\sigma_\nu' = \exp(iQ \cdot R_\nu)\sigma_\nu$ in place of σ_ν. σ_ν' may be written as a complex combination of two real vectors, u_ν and v_ν:

$$\sigma_\nu' = (u_\nu - iv_\nu)/2 \tag{2.5}$$

Then we can write (2.4) as

$$\begin{aligned}&(u_\nu \cos Q \cdot R_n + v_\nu \sin Q \cdot R_n)^2 \\ &= \tfrac{1}{2}u_\nu^2(1 + \cos 2Q \cdot R_n) + \tfrac{1}{2}v_\nu^2(1 - \cos 2Q \cdot R_n) + u_\nu \cdot v_\nu \sin 2Q \cdot R_n \\ &= 1 \quad \text{for all n and } \nu.\end{aligned} \tag{2.6}$$

Since $\sin 2Q \cdot R_n = 0$, u_ν and v_ν need not be orthogonal to each other, but since $\cos 2Q \cdot R_n = +1$ or -1 depending on R_n, they have to be unit vectors. We can also write the exchange energy (2.3) and the condition (2.4) or (2.6) as follows:

$$\varepsilon_Q = \Sigma_{\mu,\nu} C_{\mu\nu}(\pi/4)\exp[-iQ \cdot (R_\mu - R_\nu)]\sigma_\mu' \cdot \sigma_\nu'^* + c.c., \tag{2.7}$$

$$2\sigma_\nu' \cdot \sigma_\nu'^* = 1, \tag{2.8a}$$

$$\sigma_\nu'^2 + \sigma_\nu'^{*2} = 0. \tag{2.8b}$$

Under a unitary transformation

$$\begin{aligned}x_1 &= (\sigma_1' + \sigma_2' + \sigma_3' + \sigma_4')/2, \quad & x_2 &= (\sigma_1' + \sigma_2' - \sigma_3' - \sigma_4')/2, \\ x_3 &= (\sigma_1' - \sigma_2' + \sigma_3' - \sigma_4')/2, \quad & x_4 &= (\sigma_1' - \sigma_2' - \sigma_3' + \sigma_4')/2,\end{aligned} \tag{2.9}$$

eq. (2.7) becomes

$$\varepsilon_Q = 2C_{11}(\pi/4)(x_1x_1^* + x_2x_2^* + x_3x_3^* + x_4x_4^*)$$
$$+ 2\sqrt{2}C_{12}(\pi/4)(x_1x_1^* + ix_2^*x_4 - ix_2x_4^* - x_3x_3^*). \tag{2.10}$$

We see that the variables are separated into three sets: x_1, (x_2,x_4), x_3. For x_1 we obtain an eigenvalue

$$\lambda_1^{[201]}(\pi/4) = C_{11}(\pi/4) + \sqrt{2}C_{12}(\pi/4) = -2J_2(\xi - 2\eta - 2), \tag{2.11}$$

and, putting $x_2 = x_4 = x_3 = 0$, we have the corresponding eigenvector

$$u_1 = u_2 = u_3 = u_4 \equiv \hat{u}, \qquad v_1 = v_2 = v_3 = v_4 \equiv \hat{v}. \tag{2.12}$$

Here $\hat{u}$ and $\hat{v}$ are independent unit vectors. We call this spin pattern Type 1; Fig. 1 represents a special case of $u_x = u_y = v_x = v_y = 1/2$, $u_z = v_z = 1/\sqrt{2}$, which give antiferromagnetically arranged pairs of parallel-spin layers perpendicular to the x axis. For x_2 and x_4 we have

$$\begin{vmatrix} C_{11}(\pi/4) - \lambda & \sqrt{2}iC_{12}(\pi/4) \\ -\sqrt{2}iC_{12}(\pi/4) & C_{11}(\pi/4) - \lambda \end{vmatrix} = 0 \tag{2.13}$$

and hence

$$\lambda_+^{[201]}(\pi/4) = \lambda_1^{[201]}(\pi/4) \tag{2.14}$$

$$u_1 = -v_2 = -u_3 = v_4 \equiv \hat{u}', \qquad v_1 = u_2 = -v_3 = -u_4 \equiv \hat{v}', \tag{2.15}$$

where $\hat{u}'$ and $\hat{v}'$ are also independent unit vectors, and

$$\lambda_-^{[201]}(\pi/4) = C_{11}(\pi/4) - \sqrt{2}C_{12}(\pi/4) = -2J_2(-\xi + 2\eta - 2), \tag{2.16}$$

$$u_1 = v_2 = -u_3 = -v_4, \quad v_1 = -u_2 = -v_3 = u_4. \tag{2.17}$$

We call the spin pattern of eq. (2.15) Type 2. Since the eigenvalue of the Type 1 pattern is equal to that of the Type 2 pattern, it is possible to superpose the eigenvectors (2.12) and (2.15) with arbitrary amplitudes a_1 and a_2.

We express σ_ν' ($\nu = 1,2,3,4$) of eq. (2.5) as a linear combination of $(u_\nu - iv_\nu)/2$ given from (2.12) and those given from (2.15) and assume nonvanishing real a_1 and a_2,*) with $a_1^2 + a_2^2 = 1$. Then it follows from conditions (2.8a) and (2.8b) that $\hat{u}$, $\hat{v}$, $\hat{u}'$, $\hat{v}'$ are restricted in one of the following four ways:

$$\text{(a)} \quad \hat{u} = \hat{v},\ \hat{u}' \perp \hat{u},\ \hat{v}' \perp \hat{u}, \tag{2.18a}$$

$$\text{(b)} \quad \hat{u} = -\hat{v},\ \hat{u}' \perp \hat{u},\ \hat{v}' \perp \hat{u}, \tag{2.18b}$$

$$\text{(c)} \quad \hat{u}' = \hat{v}',\ \hat{u} \perp \hat{u}',\ \hat{v} \perp \hat{u}', \tag{2.18c}$$

$$\text{(d)} \quad \hat{u}' = -\hat{v}',\ \hat{u} \perp \hat{u}',\ \hat{v} \perp \hat{u}'. \tag{2.18d}$$

We call the above linearly combined spin patterns Type 3. The spin patterns of the three types may be called <u>degenerate antiferromagnetic configurations</u> and will be abbreviated as DAC.

Next, for x_3 we have

$$\lambda_3^{[201]}(\pi/4) = \lambda_-^{[201]}(\pi/4). \tag{2.19}$$

$$u_1 = -u_2 = u_3 = -u_4, \qquad v_1 = -v_2 = v_3 = -v_4. \tag{2.20}$$

The eigenvalue (2.19) is identical with (2.16) and is lower than (2.11) when $-J_2(\xi - 2\eta) > 0$, i.e., $J_0 < 2J_1$. But this case will not be considered further for the following reason.

In I we constructed spin configurations having one wavevector or two wavevectors

---

*) It is not possible to construct a real spin configuration with complex (neither real nor imaginary) amplitudes a_1 and a_2. If one of a_1 and a_2 is assumed real and the other imaginary, then we can show that the resulting spin configurations are identical with those for real a_1 and a_2; if one of a_1 and a_2 is assumed real or imaginary and the other complex (neither real nor imaginary), then we have spin configurations of (2.18a) and (2.18b) with a restriction of $\hat{u}' \perp \hat{v}'$ or those of (2.18c) and (2.18d) with a restriction of $\hat{u} \perp \hat{v}$. Thus, the assumption of real a_1 and a_2 is quite general.

restricted along [001], [110] and [111], assuming $\gamma = 0$ and taking parameter values $\zeta = J_3/J_2 = 1/2, 0, -1/2$. We studied stability regions for these configurations in the $\xi\eta$ plane, but we could not find ground spin configuration in certain regions, especially in regions where the cone-helices [110]-A and B are unstable with respect to $q = Q$. In such unstable regions we may compare the energies of [110]-A and B with the energies $\varepsilon_Q = 4\lambda_+^{[201]}(\pi/4)$ and $\varepsilon_Q = 4\lambda_-^{[201]}(\pi/4)$, assuming $\gamma = 0$ and $\zeta = 1/2, 0, -1/2$. After numerical calculations we find that $4\lambda_+^{[201]}(\pi/4)$ is lower in the case of $\zeta = 1/2$ and $J_2 < 0$, and only in this case, in the (m)-region shown in Fig. 2. On the other hand, $4\lambda_-^{[201]}(\pi/4)$ does not become lower in any case.

For this reason we confine our study to the stability of DAC in the (m)-region, and in fact its stability with respect to all wavevectors in the Brillouin zone. At first we shall solve the eigenvalue problem for the matrix $[C_{\mu\nu}(k)]$, restricting ourselves to wavevectors along [201]. Using eigenvector σ_ν in place of σ_ν', where

$$\sigma_\nu = \frac{1}{2}(\hat{i} - i\hat{j})u_\nu,$$

(see eq. (2.12) of I) and performing unitary transformation

$$\begin{aligned} X_1 &= (u_1 + u_2 + u_3 + u_4)/2, \quad & X_2 &= (u_1 + u_2 - u_3 - u_4)/2, \\ X_3 &= (u_1 - u_2 + u_3 - u_4)/2, \quad & X_4 &= (u_1 - u_2 - u_3 + u_4)/2, \end{aligned} \tag{2.22}$$

we find that the marix $[C_{\mu\nu}(k)]$ is reduced into two, corresponding to two sets: (X_1,X_4), (X_2,X_3). For (X_1,X_4) the lower eigenvalue and the corresponding eigenvector are

$$\begin{aligned} \lambda_{1-}^{[201]}(k) = \frac{1}{2}[&C_{11}(k) + C_{14}(k) + C_{22}(k) + C_{23}(k) \\ &- \sqrt{\{(C_{11}(k) + C_{14}(k) - C_{22}(k) - C_{23}(k))^2} \\ &+ 4(C_{12}(k) + C_{13}(k))^2\}], \end{aligned} \tag{2.23}$$

$$u_1 = u_4, \quad u_2 = u_3. \tag{2.24}$$

Similar ones for (X_2, X_3) are

$$\lambda_{2-}^{[201]}(k) = \frac{1}{2}[C_{11}(k) - C_{14}(k) + C_{22}(k) - C_{23}(k) - \sqrt{\{(C_{11}(k) - C_{14}(k) - C_{22}(k) + C_{23}(k))^2 + 4(C_{12}(k) - C_{13}(k))^2\}}], \tag{2.25}$$

$$u_1 = -u_4, \qquad u_2 = -u_3. \tag{2.26}$$

In order that either $d\lambda_{1-}^{[201]}(k)/dk = 0$ or $d\lambda_{2-}^{[201]}(k)/dk = 0$ at $k = \pi/4$, the following relation must hold:

$$\xi + \eta = 2\gamma + 3\zeta. \tag{2.27}$$

Thus, the stability of DAC is confined to a straight line (2.27) in the $\xi\eta$ plane for fixed values of γ and ζ.

It may be mentioned in passing that the spin configurations expressed by (2.24) and (2.26) are no real configurations. Using eqs. (2.23) and (2.24), we have

$$X_1/X_4 = (u_1 + u_2)/(u_1 - u_2) = -\frac{C_{11}(k) + C_{22}(k) + 2C_{12}(k) + 2C_{13}(k) + C_{14}(k) + C_{23}(k) - 2\lambda_{1-}^{[201]}(k)}{C_{11}(k) - C_{22}(k) + C_{14}(k) - C_{23}(k)} \tag{2.28}$$

from which it follows that

$$|u_1/u_2| \neq 1 \quad \text{for } 0 < k < \pi. \tag{2.29}$$

This implies that the configuration is not real. We have the same situation for (2.26). For the special case of $k = \pi/4$, however, the eigenvalues $\lambda_{1-}^{[201]}(k)$ and $\lambda_{2-}^{[201]}(k)$ are degenerate and hence by superposition of the corresponding eigenvectors we obtain real spin configurations. In order to construct a real helix [201] for a single eigenvalue, we must introduce parameters β_ν such that $\beta_1 = \beta_4 = \beta$, $\beta_2 = \beta_3 = 1$, which keep the symmetry of $[C_{\mu\nu}(k)]$ expressed by eq. (2.2), and study $[\beta_\mu \beta_\nu C_{\mu\nu}(k)]$. We determine β so as to satisfy the condition $|u_\nu| = 1$

for $\nu = 1,2,3,4$. After numerical calculations we find, however, that such a helix has a higher energy in the (m)-region for $\gamma = 0$, $\zeta = 1/2$, $J_2 < 0$.

Next, we study the stability of DAC with respect to other wavevectors. Because of the symmetry of $[C_{\mu\nu}(q)]$, only 1/48 of the Brillouin zone may be considered. By computer calculations we have compared the DAC eigenvalue with those for wavevectors at 125 points in the vicinity of Q. These 125 points were taken at intervals of 0.1 radian along the q_x, q_y, q_z axes around $Q = (\pi/2,0,\pi/4)$. Moreover, we have studied the stability with respect to wavevectors along [001], [110], [111] and special wavevectors at 22 points shown in Fig. 6 of I. As the final result we obtained the stability lines as shown in Fig. 3, where the assumed parameter values were $\gamma = 0.25$, 0, -0.25 and $\zeta = 0.1$, 0.2, 0.3, 0.4, 0.5, 0.6.

§3. Effect of Magnetic Dipole-Dipole Interaction

In order to find the most stable configuration, we calculate magnetic dipole-dipole energy for the degenerate antiferromagnetic configurations of Type 1, 2, 3. We determine the directions of the unit vectors $\hat{u}$, $\hat{v}$, $\hat{u}'$, and $\hat{v}'$, minimizing the dipolar energy. The dipolar energy is written as follows:

$$E_{dipole} = E_I + E_A,$$

where E_I and E_A represent the isotropic and anisotropic parts, respectively, given by

$$E_I = \frac{1}{2S^2} \Sigma_{m,\mu} \Sigma_{n,\nu} \frac{S_{m\mu} \cdot S_{n\nu}}{|R_{m\mu} - R_{n\nu}|^3} \qquad (R_{m\mu} \neq R_{n\nu}) \tag{3.1}$$

and

$$E_A = -\frac{3}{2S^2} \Sigma_{m,\mu} \Sigma_{n,\nu} \frac{\{S_{m\mu} \cdot (R_{m\mu} - R_{n\nu})\}\{S_{n\nu} \cdot (R_{m\mu} - R_{n\nu})\}}{|R_{m\mu} - R_{n\nu}|^5} \qquad (R_{m\mu} \neq R_{n\nu}). \tag{3.2}$$

Here we measure $R_{n\nu}$ in units of $a/4$ and the dipolar energy in units of $(g\mu_B S)^2/(a/4)^3 = 1.162\text{cm}^{-1}$ ($gS = 5$, $a = 8.416\text{Å}$).

The configuration of Type 3 is given as a superposition of the eigenvector (2.12) for Type 1 and the eigenvector (2.15) for Type 2, with arbitrary real amplitudes a_1 and a_2. The corresponding spin vectors are expressed as

$$\begin{aligned}
S_{n1} &= S[a_1(\hat{u}\cos Q\cdot R_n + \hat{v}\sin Q\cdot R_n) + a_2(\hat{u}'\cos Q\cdot R_n + \hat{v}'\sin Q\cdot R_n)], \\
S_{n2} &= S[a_1(\hat{u}\cos Q\cdot R_n + \hat{v}\sin Q\cdot R_n) + a_2(-\hat{u}'\sin Q\cdot R_n + \hat{v}'\cos Q\cdot R_n)], \\
S_{n3} &= S[a_1(\hat{u}\cos Q\cdot R_n + \hat{v}\sin Q\cdot R_n) + a_2(-\hat{u}'\cos Q\cdot R_n - \hat{v}'\sin Q\cdot R_n)], \\
S_{n4} &= S[a_1(\hat{u}\cos Q\cdot R_n + \hat{v}\sin Q\cdot R_n) + a_2(\hat{u}'\sin Q\cdot R_n - \hat{v}'\cos Q\cdot R_n)].
\end{aligned} \tag{3.3}$$

Type 1 corresponds to $a_1 = 1$, $a_2 = 0$ and Type 2 to $a_1 = 0$, $a_2 = 1$. For (3.3) the energies given by eqs. (3.1) and (3.2) are represented as linear combinations of following lattice sums:

$$I^{(c)}_{m\mu\nu} = \Sigma_n \frac{\cos Q\cdot R_n}{|R_{m\mu} - R_{n\nu}|^3}, \tag{3.4a}$$

$$I^{(s)}_{m\mu\nu} = \Sigma_n \frac{\sin Q\cdot R_n}{|R_{m\mu} - R_{n\nu}|^3}, \tag{3.4a}$$

$$A^{(c)}_{m\mu\nu\alpha\beta} = -3\Sigma_n \frac{(R_{m\mu\alpha} - R_{n\nu\alpha})(R_{m\mu\beta} - R_{n\nu\beta})\cos Q\cdot R_n}{|R_{m\mu} - R_{n\nu}|^5}, \tag{3.5a}$$

$$A^{(s)}_{m\mu\nu\alpha\beta} = -3\Sigma_n \frac{(R_{m\mu\alpha} - R_{n\nu\alpha})(R_{m\mu\beta} - R_{n\nu\beta})\sin Q\cdot R_n}{|R_{m\mu} - R_{n\nu}|^5}, \tag{3.5b}$$

where α and β represent cartesian components. We choose a magnetic unit cell having basis vectors of lengths a, a, 2a (i.e., 4, 4, 8 in units of a/4) along the x, y, z axes. This unit cell contains eight rhombohedral chemical unit cells. The origins of these eight chemical unit cells are chosen at

$$(0,0,0),\ (2,2,0),\ (2,0,\pm 2),\ (0,2,\pm 2),\ (0,0,4),\ (2,2,4).$$

Correspondingly, we have eight R_m $(=R_{m\mu} - R_{0\mu})$ in eqs. (3.1) and (3.2) as well as in eqs. (3.4a) $\sim$ (3.5b). In carring out summations in eqs. (3.1) and (3.2) we at first take sum over eight vectors and then multiply the result by the number of magnetic unit cells. Writting $R_m = (0,0,0) \equiv R_a$, we have relations given by eqs. (A.1) $\sim$ (A.13) in Appendix A for $I^{(c)}_{a\mu\nu}$, $I^{(s)}_{a\mu\nu}$, $A^{(c)}_{a\mu\nu\alpha\beta}$ and $A^{(s)}_{a\mu\nu\alpha\beta}$. Furthermore, writting $R_m = (0,2,2) \equiv R_b$, we obtain following relations:

$$I^{(c)}_{b\mu\nu} = -I^{(s)}_{a\mu\nu}, \qquad I^{(s)}_{b\mu\nu} = I^{(c)}_{a\mu\nu}, \tag{3.6}$$

$$A^{(c)}_{b\mu\nu\alpha\beta} = -A^{(s)}_{a\mu\nu\alpha\beta}, \qquad A^{(s)}_{b\mu\nu\alpha\beta} = A^{(c)}_{a\mu\nu\alpha\beta}. \tag{3.7}$$

The lattice sums $I^{(c)}_{m\mu\nu}$, $I^{(s)}_{m\mu\nu}$, $A^{(c)}_{m\mu\nu\alpha\beta}$, $A^{(s)}_{m\mu\nu\alpha\beta}$ for other m's are related to those for a or b in the way shown in Appendix A. After calculations we obtain the following expression for the total dipolar energy:

$$E_{dipole}/4N = I + a_1^2[\tfrac{1}{2}A_1(u_x^2 + u_y^2 + v_x^2 + v_y^2) + \tfrac{1}{2}A_2(u_z^2 + v_z^2)]$$
$$+ a_2^2[\tfrac{1}{2}A_1(u_x'^2 + u_y'^2 + v_x'^2 + v_y'^2) + \tfrac{1}{2}A_2(u_z'^2 + v_z'^2)]$$

$$+ a_1 a_2 [\tfrac{1}{2} A_3 (u_x u_z' - u_x v_z' + v_x u_z' + v_x v_z' + u_z u_x' - u_z v_x' + v_z u_x' + v_z v_x'$$

$$+ u_y u_z' + u_y v_z' - v_y u_z' + v_y v_z' + u_z u_y' + u_z v_y' - v_z u_y' + v_z v_y')], \quad (3.8)$$

where

$$I = \tfrac{1}{2}(I_{a11}^{(c)} + 2I_{a12}^{(c)}), \quad (3.9)$$

$$A_1 = \tfrac{1}{2}(A_{a11xx}^{(c)} + A_{a12xx}^{(c)} + A_{a12yy}^{(c)}), \quad (3.10)$$

$$A_2 = \tfrac{1}{2}(A_{a11zz}^{(c)} + 2A_{a12zz}^{(c)}), \quad (3.11)$$

$$A_3 = \tfrac{1}{2}(A_{a13xz}^{(s)} + 2A_{a12yz}^{(c)}). \quad (3.12)$$

We carried out computer calculations and obtained following numerical results:

$$I = 0.178 \ (= 0.207 \ \text{cm}^{-1}), \quad (3.13)$$

$$A_1 = -0.051 \ (= -0.059 \ \text{cm}^{-1}),$$

$$A_2 = -0.453 \ (= -0.526 \ \text{cm}^{-1}), \quad (3.14)$$

$$A_3 = -0.677 \ (= -0.787 \ \text{cm}^{-1}).$$

We minimize the dipolar energy (3.8), subject to conditions $a_1^2 + a_2^2 = 1$ and

$$u_x^2 + u_y^2 + u_z^2 = 1, \qquad v_x^2 + v_y^2 + v_z^2 = 1, \quad (3.15)$$

$$u_x'^2 + u_y'^2 + u_z'^2 = 1, \quad v_x'^2 + v_y'^2 + v_z'^2 = 1. \quad (3.16)$$

At first we put either $a_1 = 1$, $a_2 = 0$ or $a_1 = 0$, $a_2 = 1$ (Type 1 or Type 2) and obtain the same minimum dipolar energy

$$E_{dipole}/4N = I + A_2 = -0.320 \ \text{cm}^{-1}. \quad (3.17)$$

The corresponding eigenvector is

$$u_x = u_y = v_x = v_y = 0, \qquad u_z^2 = 1, \qquad v_z^2 = 1. \quad (3.18)$$

or

$$u_x' = u_y' = v_x' = v_y' = 0, \quad u_z'^2 = 1, \quad v_z'^2 = 1. \tag{3.19}$$

Hence, in both cases the spin axis in the minimum energy configuration is parallel to the z axis. Next we consider Type 3 ($a_1 \neq 0$, $a_2 \neq 0$) which must satisfy one of the four conditions (2.18a) $\sim$ (2.18d). We show in Appendix B the details of solving the minimum problem for example in the case of (2.18a) ($\hat{u} = \hat{v}$, $\hat{u}' \perp \hat{u}$, $\hat{v}' \perp \hat{u}$).

Case (a)

In the case of (2.18a) we obtain the minimum dipolar energy as

$$E_{dipole}/4N = I + 0.642A_2 + 0.358A_1 + 0.959A_3$$
$$= -0.906 \text{ cm}^{-1}, \tag{3.20}$$

with amplitudes $a_1 = 0.802$ and $a_2 = 0.598$ for the eigenvectors

$$u_x = u_y = v_x = v_y = 0, \quad u_z = v_z = 1,$$
$$u_x' = v_y' = 1, \quad u_y' = u_z' = v_x' = v_z' = 0. \tag{3.21a}$$

In the remaining three cases we obtain the same dipolar energy as (3.20), with following amplitudes of the eigenvectors:

Case (b)

$a_1 = 0.802$. $a_2 = 0.598$ for

$$u_x = u_y = v_x = v_y = 0, \quad u_z = -v_z = 1,$$
$$u_y' = -v_x' = 1, \quad u_x' = u_z' = v_y' = v_z' = 0. \tag{3.21b}$$

Case (c)

$a_1 = 0.598$, $a_2 = 0.802$ for

$$u_y = v_x = 1, \quad u_x = u_z = v_y = v_z = 0,$$
$$u_x' = u_y' = v_x' = v_y' = 0, \quad u_z' = v_z' = 1. \tag{3.21c}$$

Case (d)

$a_1 = 0.598$, $a_2 = 0.802$ for

$$u_x = -v_y = 1, \quad u_y = u_z = v_x = v_z = 0,$$

$$u_x' = u_y' = v_x' = v_y' = 0, \quad u_z' = -v_z' = 1. \tag{3.21d}$$

We have shown above that the four noncollinear configurations of Type 3 have the same lowest dipolar energy given by (3.20). In the case of $ZnFe_2O_4$ there may be an anisotropy energy due to crystalline field. The cubic spin Hamiltonian for Fe^{3+} ($S = 5/2$) is represented by

$$\frac{a}{6}(S_x^4 + S_y^4 + S_z^4),$$

where $a \simeq 2.0 \times 10^{-2}$ cm^{-1}.[3] This anisotropy energy is by two orders of magnitude smaller than (3.20) and hence can be neglected.

The four spin configurations of the lowest dipolar energy are shown in Fig. 4 (a), (b), (c), and (d), respectively; (a) and (b) are related by a mirror plane $(1\bar{1}0)$, as are (c) and (d).

§4. Discussion

Assuming a special wavevector $Q = (2\pi/a, 0, \pi/a)$ we have obtained degenerate antiferromagnetic configurations (DAC) of Type 1 and Type 2, and their superposition Type 3. It was shown that these configurations are stable on that part of the line (2.27) in the $\xi\eta$ plane ($\xi = J_0/J_2$, $\eta = J_1/J_2$) which is within the region denoted by (m) in Fig. 2 (which is for the case of $\zeta = 1/2$) for γ $(= \frac{J_2'' - J_2'}{2J_2})$ = const and ζ $(= J_3/J_2)$ = const. Our numerical computations predicted that this line exists only for $\zeta > 0$ and $J_2 < 0$, or $J_3 < 0$ and $J_2 < 0$; cases other than $\zeta = 1/2$ are shown by Fig. 3. The stability was proved by checking that for these configurations the eigenvalue of exchange matrix is the lowest of all eigenvalues of the matrix with wavevector varying over the whole Brillouin zone. This provides a sufficient, but not necessary, condition for the stability.

We have made an attempt to construct a helical spin configuration having a single wavevector q of arbitrary magnitude along [201] and corresponding to a single eigenvalue. It was found that such a helical spin configuration has a much higher exchange energy at $q = Q$ and $q \simeq Q$ than the degenerate antiferromagnetic configurations having $q = Q$. This situation arises from the fact that we obtain degenerate eigenvalues only for $q = Q$ but not for $q \neq Q$, so that we obtain real spin configurations for $q = Q$ without introducing parameters β_ν into the exchange matrix, whereas for $q \neq Q$ we have to introduce β_ν and determine them so as to obtain a real helical spin configuration.

There exist two kinds of helical spin configuration for $q = (2k, 0, k)$ with $k \neq \pi/a$ which tend for $k \to \pi/a$ to one of the degenerate antiferromagnetic configurations that we have found for $q = Q$. They are as follows:

(1) Helix [201]-1

$$S_{n\nu} = S[\hat{u}\cos(2kR_{nx} + kR_{nz}) + \hat{v}\sin(2kR_{nx} + kR_{nz})], \qquad (4.1)$$

where $\hat{u} \perp \hat{v}$. The exchange energy is written as

$$E_{ex}/NS^2 = 2[C_{11}(k) + C_{22}(k) + 2C_{12}(k)\cos k + 2C_{13}(k)\cos 2k + C_{14}(k)\cos 3k + C_{23}(k)\cos k]. \quad (4.2)$$

Helix [201]-1 tends to Type 1 with $\hat{u} \perp \hat{v}$ for $k \to \pi/4$ (in units of $4/a$).

(2) Helix [201]-2

$$\begin{aligned} S_{n1} &= S[\hat{u}'\cos(2kR_{nx} + kR_{nz}) + \hat{v}'\sin(2kR_{nx} + kR_{nz})], \\ S_{n2} &= S[-\hat{u}'\sin(2kR_{nx} + kR_{nz}) + \hat{v}'\cos(2kR_{nx} + kR_{nz})], \\ S_{n3} &= S[-\hat{u}'\cos(2kR_{nx} + kR_{nz}) - \hat{v}'\sin(2kR_{nx} + kR_{nz})], \\ S_{n4} &= S[\hat{u}'\sin(2kR_{nx} + kR_{nz}) - \hat{v}'\cos(2kR_{nx} + kR_{nz})], \end{aligned} \quad (4.3)$$

where $\hat{u}' \perp \hat{v}'$. The exchange energy is

$$E_{ex}/NS^2 = 2[C_{11}(k) + C_{22}(k) + 2C_{12}(k)\sin k - 2C_{13}(k)\cos 2k - C_{14}(k)\sin 3k + C_{23}(k)\sin k]. \quad (4.4)$$

Helix [201]-2 tends to Type 2 with $\hat{u}' \perp \hat{v}'$ for $k \to \pi/4$.

The exchange energies (4.2) and (4.4) have a minimum value at $k = \pi/4$ which agrees with the exchange energy of DAC, not only on the straight line (2.27) but also out of it. It is therefore possible that DAC has stability in some region which includes the straight line, although we could not give a rigorous proof for this expectation. By looking for the configuration of the lowest dipolar energy out of the degenerate antiferromagnetic configurations we may expect at least that this configuration of the lowest dipolar energy will have stability that contains the mentioned straight line.

The spin configuration of the minimum dipolar energy will be the spin configuration of $ZnFe_2O_4$ at $T = 0$. We expect that the exchange constants of $ZnFe_2O_4$ will approximately, if not exactly, satisfy the relation (2.27), or $J_0 + J_1 + J_2' = J_2'' + 3J_3$, as well as inequalities $J_2 < 0$, $J_3 < 0$, and $J_0 > 2J_1$ ($\xi - 2\eta < 0$); more specifically, we expect that the exchange constants will fall near one of the finite lines shown in Fig. 3. By a neutron diffraction study of $ZnFe_2O_4$

König et al. proposed three possible spin configurations. One is a collinear antiferromagnetic configuration with $u_x = u_y = v_x = v_y = 1/2$ and $u_z = v_z = 1/\sqrt{2}$ (Fig. 1). The second is a noncollinear antiferromagnetic configuration of our Type 3 having $\hat{u} = \hat{v} = \hat{z}$, $\hat{u}' = \hat{x}$, $\hat{v}' = \hat{y}$, and $a_1 = a_2 = 1/\sqrt{2}$. For these two configurations the equantity

$$R = \Sigma |I_{obs} - I_{cal}| / \Sigma I_{obs}, \tag{4.5}$$

which measures the deviation of the calculated line intensities from those observed, takes a value of 5.5%. This value was obtained for a low magnetic moment value of $3.9\mu_B$ at 4.2K. The third configuration corresponds to our Type 2 with $\hat{u}' = \hat{x}$ and $\hat{v}' = \hat{y}$, for which the R value is 6.2% and the magnetic moment value is $4.2\mu_B$ at 4.2K. (They argued that the low magnetic moment values are due to covalency effect and that if $\hat{u} = \hat{v} = \hat{z}$ is assumed in the Type 1 configuration, then R will amount to 11%.) The second spin configuration proposed by König et al. comes close to one of our spin configurations of the minimum dipolar energy which is expressed by (3.21a). Our four possible spin configurations give the same powder line intensities listed in Table 1. It may be mentioned that the magnetic form factor we obtain from the calculated line intensities of König et al. for the first and second configurations do not agree with that we obtain from those for third configuration, and hence our R value for the four configurations is 8.45% using the former form factor and 8.12% using the latter form factor (a low magnetic moment $3.9\mu_B$ is assumed).

Appendix A: Relations Among Lattice Sums

Relations among the lattice sums defined by eqs. (3.4a), (3.4b), (3.5a), and (3.5b) for $R_m = (0,0,0) \equiv R_a$ are as follows:

$$I^{(c)}_{a\mu\mu} = \underline{I^{(c)}_{a11}}, \qquad I^{(s)}_{a\mu\mu} = 0, \qquad \text{for } \mu = 1,2,3,4. \tag{A.1}$$

$$I^{(c)}_{a\mu\nu} = I^{(c)}_{a\nu\mu}, \qquad I^{(s)}_{a\mu\nu} = -I^{(s)}_{a\nu\mu}, \qquad \text{for } \mu \neq \nu. \tag{A.2}$$

$$I^{(c)}_{a14} = I^{(s)}_{a14} = I^{(c)}_{a23} = -I^{(s)}_{a23} = I^{(c)}_{a34} = -I^{(s)}_{a34} = -I^{(s)}_{a12} = \underline{I^{(c)}_{a12}}. \tag{A.3}$$

$$I^{(c)}_{a13} = I^{(s)}_{a13} = I^{(c)}_{a24} = I^{(s)}_{a24} = 0. \tag{A.4}$$

$$A^{(c)}_{a\mu\mu xx} = A^{(c)}_{a\mu\mu yy} = \underline{A^{(c)}_{a11xx}}, \qquad A^{(c)}_{a\mu\mu zz} = \underline{A^{(c)}_{a11zz}},$$

$$A^{(c)}_{a\mu\mu\alpha\beta} = 0 \ (\alpha \neq \beta), \qquad A^{(s)}_{a\mu\mu\alpha\beta} = 0, \qquad \text{for } \mu = 1,2,3,4. \tag{A.5}$$

$$A^{(c)}_{a\mu\nu\alpha\beta} = A^{(c)}_{a\nu\mu\alpha\beta}, \qquad A^{(s)}_{a\mu\nu\alpha\beta} = -A^{(s)}_{a\nu\mu\alpha\beta}, \qquad \text{for } \alpha \neq \beta, \ \mu \neq \nu. \tag{A.6}$$

$$A^{(c)}_{a\mu\nu\alpha\beta} = A^{(c)}_{a\mu\nu\beta\alpha}, \qquad A^{(s)}_{a\mu\nu\alpha\beta} = A^{(s)}_{a\mu\nu\beta\alpha}, \qquad \text{for } \alpha \neq \beta, \ \mu \neq \nu. \tag{A.7}$$

$$A^{(c)}_{a14yy} = A^{(s)}_{a14yy} = A^{(c)}_{a23yy} = -A^{(s)}_{a23yy} = A^{(c)}_{a34xx} = -A^{(s)}_{a34xx} = -A^{(s)}_{a12xx} = \underline{A^{(c)}_{a12xx}}. \tag{A.8}$$

$$A^{(c)}_{a14xx} = A^{(s)}_{a14xx} = A^{(c)}_{a23xx} = -A^{(s)}_{a23xx} = A^{(c)}_{a34yy} = -A^{(s)}_{a34yy} = -A^{(s)}_{a12yy} = \underline{A^{(c)}_{a12yy}}. \tag{A.9}$$

$$A^{(c)}_{a14xz} = A^{(s)}_{a14xz} = -A^{(c)}_{a23xz} = A^{(s)}_{a23xz} = -A^{(c)}_{a34yz} = A^{(s)}_{a34yz} = -A^{(s)}_{a12yz} = \underline{A^{(c)}_{a12yz}}. \tag{A.10}$$

$$A^{(c)}_{a14zz} = A^{(s)}_{a14zz} = A^{(c)}_{a23zz} = -A^{(s)}_{a23zz} = A^{(c)}_{a34zz} = -A^{(s)}_{a34zz} = -A^{(s)}_{a12zz} = \underline{A^{(c)}_{a12zz}}. \tag{A.11}$$

$$A^{(s)}_{a24xz} = A^{(s)}_{a24yz} = -A^{(s)}_{a13yz} = \underline{A^{(s)}_{a13xz}}. \tag{A.12}$$

$$A^{(c)}_{a13\alpha\alpha} = A^{(s)}_{a13\alpha\alpha} = A^{(c)}_{a24\alpha\alpha} = A^{(s)}_{a24\alpha\alpha} = 0, \qquad \text{for } \alpha = x,y,z,$$

$$A^{(c)}_{a\mu\nu xy} = A^{(s)}_{a\mu\nu xy} = 0, \qquad \text{for all } \mu \text{ and } \nu,$$

$$A^{(c)}_{a12xz} = A^{(s)}_{a12xz} = A^{(c)}_{a34xz} = A^{(s)}_{a34xz} = A^{(c)}_{a14yz} = A^{(s)}_{a14yz} = A^{(c)}_{a23yz} = A^{(s)}_{a23yz}$$

$$= A^{(c)}_{a13xz} = A^{(c)}_{a13yz} = A^{(c)}_{a24xz} = A^{(c)}_{a24yz} = 0. \tag{A.13}$$

For $R_m = (2,2,4)$ we have

$$I^{(c)}_{m\mu\nu} = I^{(c)}_{a\mu\nu}, \qquad I^{(s)}_{m\mu\nu} = I^{(s)}_{a\mu\nu},$$

$$A^{(c)}_{m\mu\nu\alpha\beta} = A^{(c)}_{a\mu\nu\alpha\beta}, \qquad A^{(s)}_{m\mu\nu\alpha\beta} = A^{(s)}_{a\mu\nu\alpha\beta}. \tag{A.14}$$

For $R_m = (2,0,-2)$ we have similar relations with suffix b in place of a. For $R_m = (2,2,0)$ and $(0,0,4)$ we have

$$I^{(c)}_{m\mu\nu} = -I^{(c)}_{a\mu\nu}, \qquad I^{(s)}_{m\mu\nu} = -I^{(s)}_{a\mu\nu},$$
$$A^{(c)}_{m\mu\nu\alpha\beta} = -A^{(c)}_{a\mu\nu\alpha\beta}, \qquad A^{(s)}_{m\mu\nu\alpha\beta} = -A^{(s)}_{a\mu\nu\alpha\beta}. \tag{A.15}$$

For $R_m = (0,2,-2)$ and $(2,0,2)$ we have similar relations with suffix b in place of a.

Appendix B: Method of Finding Minimum of Dipolar Energy

In the case (a) in §3 the following conditions must be satisfied:

$$\hat{u} = \hat{v}, \tag{B.1}$$

$$\hat{u}' \perp \hat{u}, \qquad \hat{v}' \perp \hat{u}, \tag{B.2}$$

$$u_x^2 + u_y^2 + u_z^2 = 1, \tag{B.3}$$

$$u_x'^2 + u_y'^2 + u_z'^2 = 1, \qquad v_x'^2 + v_y'^2 + v_z'^2 = 1, \tag{B.4}$$

$$a_1^2 + a_2^2 = 1. \tag{B.5}$$

Using eq. (B.1), we have the dipolar energy

$$E_{dipole}/4N = a_1^2[A_1(u_x^2 + u_y^2) + A_2 u_z^2] + a_2^2[\tfrac{1}{2}A_1(u_x'^2 + u_y'^2 + v_x'^2 + v_y'^2) + \tfrac{1}{2}A_2(u_z'^2 + v_z'^2)] + a_1 a_2 A_3(u_x u_z' + u_z u_x' + u_y v_z' + u_z v_y'). \tag{B.6}$$

Neglecting (B.2) for a moment, we confine ourselves to conditions (B.3) and (B.4). We introduce a set of Lagrangian multiplies $\{\lambda_\phi\}$, $\phi = u,u',v'$, and put

$$\lambda_u = \lambda, \qquad \lambda_{u'} = \lambda_{v'} = \lambda/\delta^2. \tag{B.7}$$

Then, for minimizing (B.6) we obtain eigenvalue equations as follows.

For (u_z, u_x', v_y') the equation is

$$\begin{vmatrix} 2a_1^2A_2 - 2\lambda & a_1a_2A_3 & a_1a_2A_3 \\ a_1a_2A_3 & a_2^2A_1 - 2\lambda/\delta^2 & 0 \\ a_1a_2A_3 & 0 & a_2^2A_1 - 2\lambda/\delta^2 \end{vmatrix} = 0. \tag{B.8}$$

The lowest root is

$$\lambda_1 = \tfrac{1}{4}[\delta^2 a_2^2 A_1 + 2a_1^2 A_2 - \sqrt{\{(\delta^2 a_2^2 A_1 - 2a_1^2 A_2)^2 + 8\delta^2 a_1^2 a_2^2 A_3^2\}}], \tag{B.9}$$

and the next root is

$$\lambda_2 = \delta^2 a_2^2 A_1/2. \tag{B.10}$$

For (u_x, u_z') or (u_y, v_z') we have

$$\begin{vmatrix} 2a_1^2A_1 - 2\lambda & a_1a_2A_3 \\ a_1a_2A_3 & a_2^2A_2 - 2\lambda/\delta^2 \end{vmatrix} = 0 \qquad (B.11)$$

whose lower root is

$$\lambda_3 = \frac{1}{4}[\delta^2a_2^2A_2 + 2a_1^2A_1 - \sqrt{\{(\delta^2a_2^2A_2 - 2a_1^2A_1)^2 + 4\delta^2a_1^2a_2^2A_3^2\}}]. \qquad (B.12)$$

Furthermore, for u_y' or v_x' we have

$$\lambda_4 = \lambda_2 = \delta^2a_2^2A_1/2. \qquad (B.13)$$

If we take the eigenvalue λ_1, then we have to put

$$u_x = u_y = u_y' = u_z' = v_x' = v_z' = 0, \qquad (B.14)$$

which means that the condition (B.2) is satisfied. Furthermore, we choose δ^2 in such a way that equations (B.3) and (B.4) are satisfied, i.e.,

$$u_z = u_x' = v_y' = 1, \qquad (B.15)$$

is satisfied. Then it follows that

$$\delta^2 = 2(a_1^2A_2 + a_1a_2A_3)/(a_2^2A_1 + a_1a_2A_3). \qquad (B.16)$$

Using this δ^2, we minimize λ_1 of eq. (B.9) with respect to amplitude a_1 or a_2 which are subject to condition (B.5). After numerical calculations we obtain

$$a_1 = 0.802, \quad a_2 = 0.598, \qquad (B.17)$$

and the corresponding minimum dipolar energy

$$E_{dipole}/4N = I + 0.642A_2 + 0.358A_1 + 0.959A_3 = -0.906\ cm^{-1}, \qquad (B.18)$$

For λ_3 we have

$$u_z = u_x' = u_y' = v_x' = v_y' = 0, \qquad (B.19)$$

so that (B.2) is again satisfied. We then choose δ^2 in such a way that

$$u_x = u_y = 1/\sqrt{2}, \quad u_z' = v_z' = 1 \qquad (B.20)$$

are satisfied. Numerical calculations show that the corresponding dipolar energy is higher than (B.18). The configuration with the eigenvalue (B.13) also has a higher dipolar energy.

References

1) J. M. Hastings and L. M. Coliss: Phys. Rev. 102, 1460 (1956).

2) U. König, E. F. Bertaut, Y. Gros, M. Mitrikov and G. Chol: Solid State Communications 8, 759 (1970).

3) K. Yosida and M. Tachiki: Prog. Theor. Phys. 17, 331 (1957).

Table 1. Magnetic Intensities

h k l[A)]	Observed Intensities	Calculated Intensities			
		König et al.		present paper	
		second[B)] (Type 3) $3.9\mu_B$	third[C)] (Type 2) $4.2\mu_B$	M.F.F. from second[D)] $3.9\mu_B$	M.F.F. from third[E)] $3.9\mu_B$
001	7400	7611	7406	7923	7923
211	500	453	365	491	491
213 015	1700	1638	1902	1628	1628
031	650	605	475	658	658
233 035	500	596	557	626	626
037 019	400	238	427	199	199
431 051 237 219	360	377	308	399	367
251 417 039	250	243	320	233	235
$R=\Sigma \lvert I_{obs}-I_{cal} \rvert / \Sigma I_{obs}$		5.5%	6.2%	8.45%	8.12%

A) Indices h, k, l refer to the magnetic unit cell (a,a,2a).

B) Calculated line intensities for the second configuration, $u_z = v_z = 1$, $u_x' = v_y' = 1$, $a_1 = a_2 = 1/\sqrt{2}$.

C) Calculated line intensities for the third configuration, $u_x' = v_y' = 1$.

D) Calculated line intensities for the four configurations of the lowest dipolar energy using the magnetic form factor (M.F.F.) recalculated from line intensities of the second configuration.

E) Same as D) but using the magnetic form factor recalculated from intensities of the third configuration.

Fig. 1. The spin configuration of Type 1. The case of $u_x = u_y = v_x = v_y = 1/2$, $u_z = v_z = 1/\sqrt{2}$ is shown. Open circles mean +z components and full circles -z components. A translation (0,0,a) reverses all spins.

Fig. 2. Region of lower energy of the degenerate antiferromagnetic configurations (DAC), denoted by (m), in the case of $\gamma = 0$, $\zeta = J_3/J_2 = 1/2$, $J_2 < 0$. Here $\xi = J_0/J_2$, $\eta = J_1/J_2$. The helix [001]-2 is denoted by (c), uncorrelated antiferromagnetic configuration-2 by (f) (see Sec. 3 of I). Shaded region mean the regions of unkown ground state spin configurations.

Fig. 3. Stability lines of DAC for fixed values of γ and ζ in the case of $J_2 < 0$. Assumed parameter values are $\gamma = 0.25$, 0, -0.25 and $\zeta = 0.1$, 0.2, 0.3, 0.4, 0.5, 0.6.

Fig. 4. The four spin configurations of Type 3 of the lowest dipolar energy, which are predicted as spin configurations in $ZnFe_2O_4$.

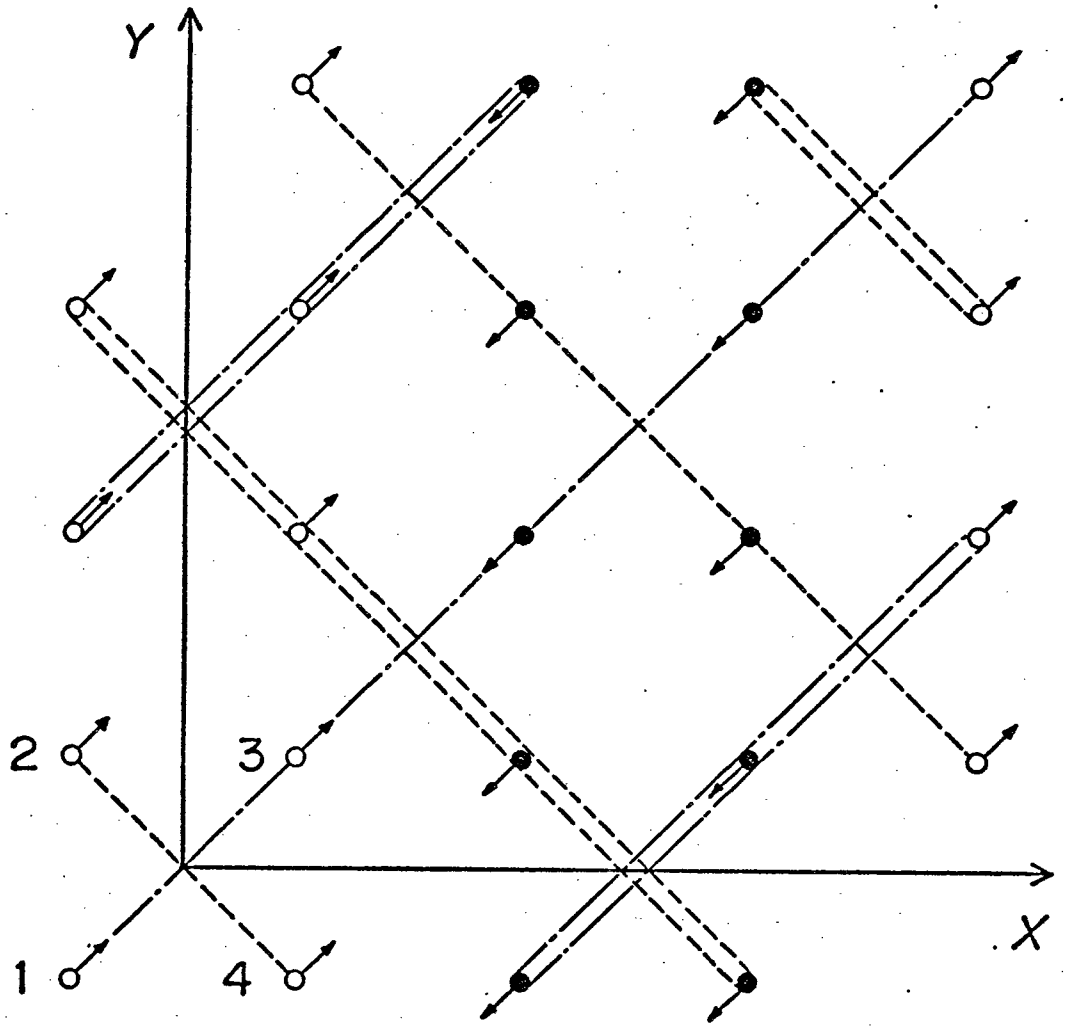

$Z=-\frac{a}{8}$ $Z=0$

$Z=\frac{a}{8}$ $Z=\frac{3a}{8}$

$Z=\frac{5a}{8}$ ○ up ● down

Fig. 1

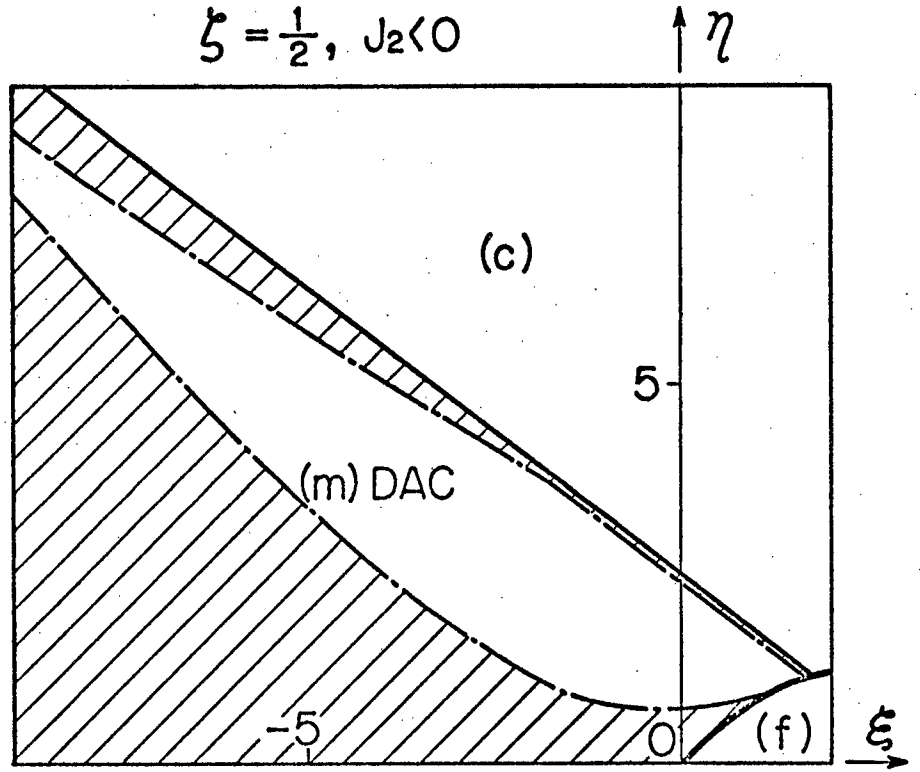

Fig. 2

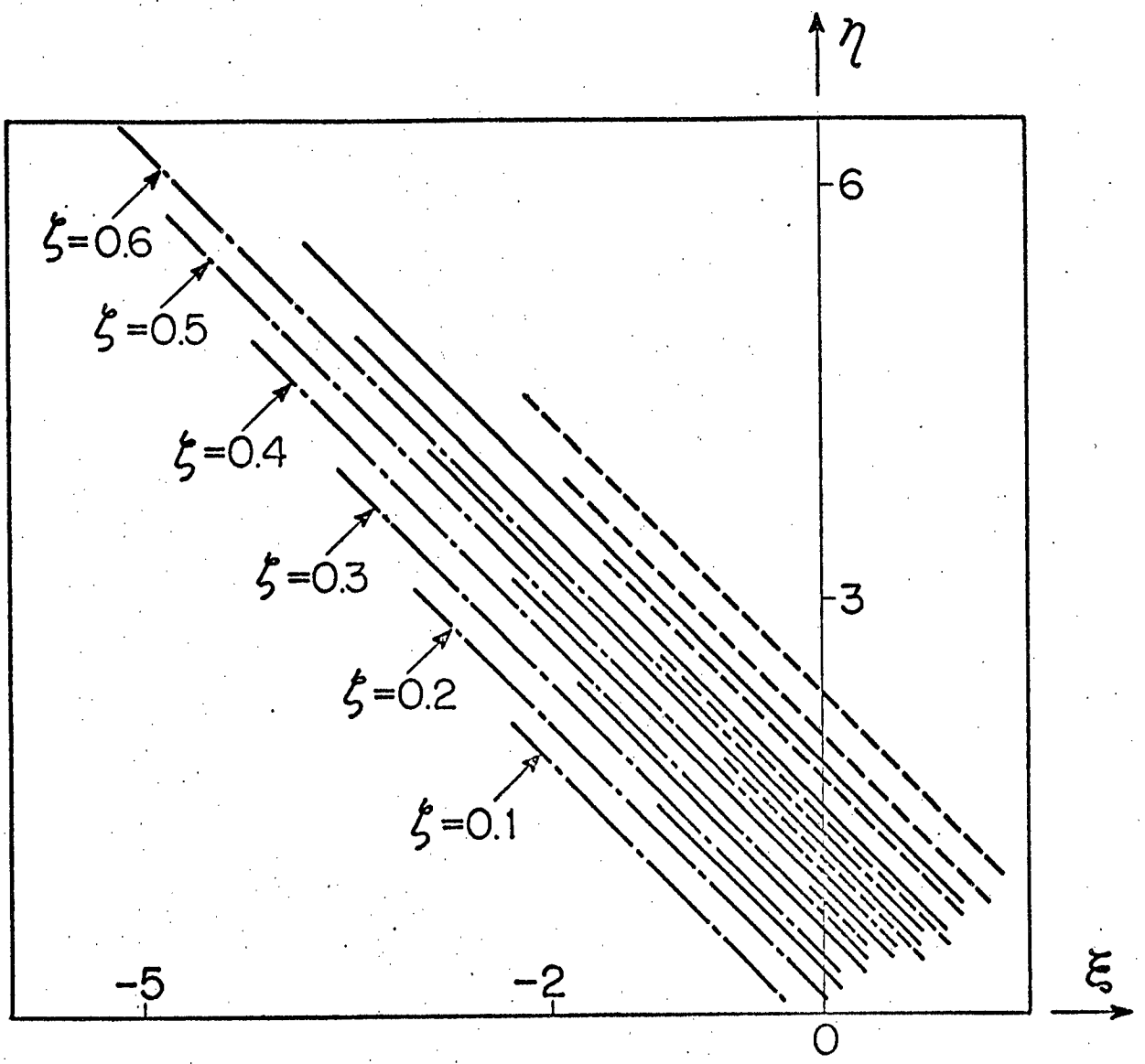

Fig. 3

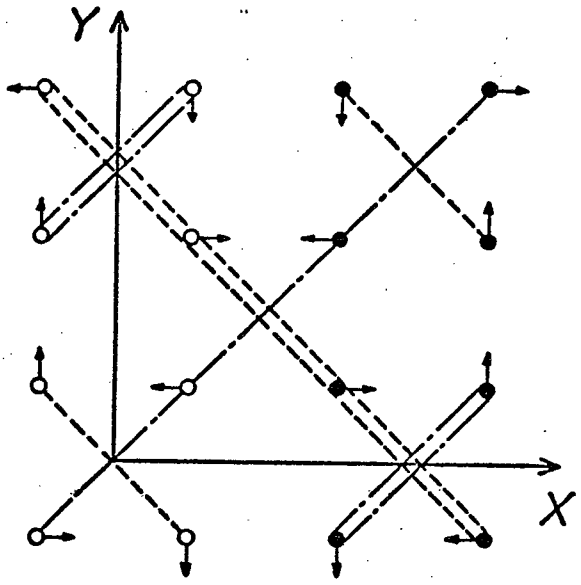

(a)

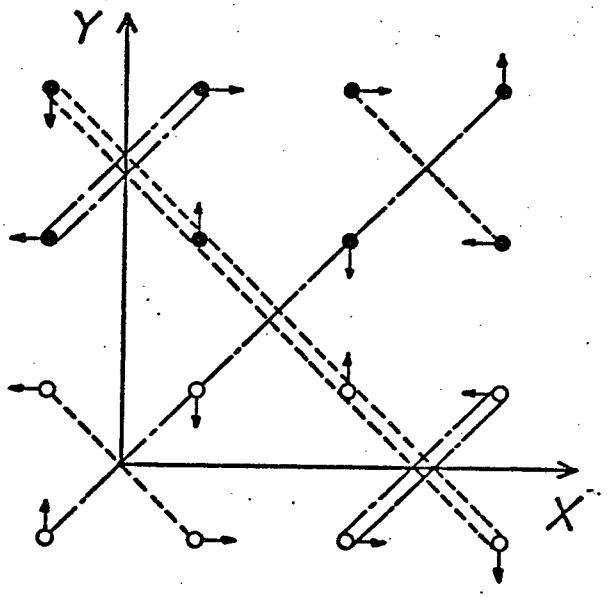

(b)

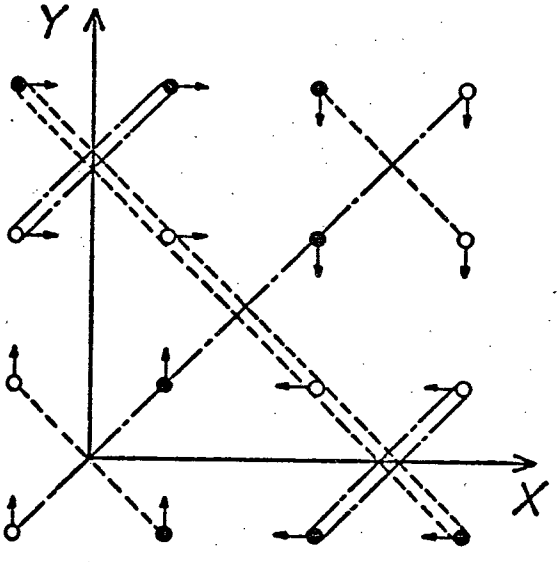

(c)

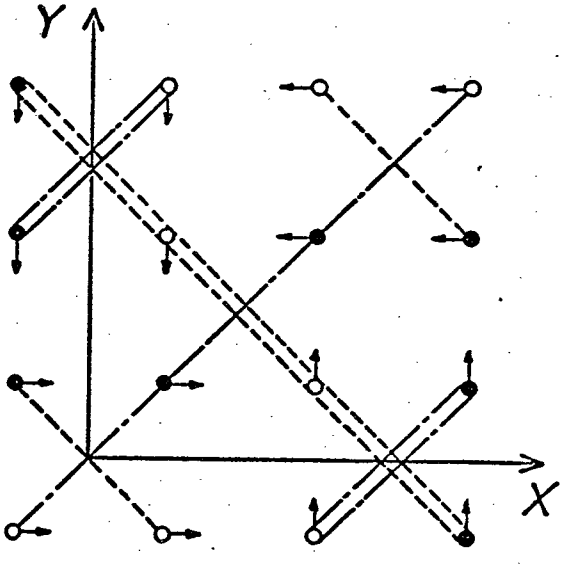

(d)

$Z=-\frac{a}{8}$ $Z=0$

$Z=\frac{a}{8}$ $Z=\frac{3a}{8}$

$Z=\frac{5a}{8}$ ○ up ● down

Fig. 4

論 文 目 録

大阪大學

報告番号	甲第1636号	氏名	秋濃俊郎

主論文　Spin Configurations of Magnetic Ions on B-Sites in Normal Cubic Spinels

（正スピネル構造のB位置における磁性イオンのスピン配列）

欧文題名　Spin Configurations of Magnetic Ions on B-Sites in Normal Cubic Spinels

（正スピネル構造のB位置における磁性イオンのスピン配列）

Journal of The Physical Society of Japan, Vol. 31, No. 3, P. 691～705, September, 1971

欧文題名　Theory of Magnetic Structure of Zinc Ferrite

（亜鉛フェライトの磁気構造の理論）

to be published in Journal of The Physical Society of Japan, Vol. 36, No. 1, January, 1974